



New hybridized mixed methods for linear elasticity and optimal multilevel solvers

Shihua Gong¹ · Shuonan Wu² · Jinchao Xu²

Received: 25 April 2017 / Revised: 27 March 2018 / Published online: 24 October 2018
© Springer-Verlag GmbH Germany, part of Springer Nature 2018

Abstract

In this paper, we present a family of new mixed finite element methods for linear elasticity for both spatial dimensions $n = 2, 3$, which yields a conforming and strongly symmetric approximation for stress. Applying $\mathcal{P}_{k+1} - \mathcal{P}_k$ as the local approximation for the stress and displacement, the mixed methods achieve the optimal order of convergence for both the stress and displacement when $k \geq n$. For the lower order case ($n - 2 \leq k < n$), the stability and convergence still hold on some special grids. The proposed mixed methods are efficiently implemented by hybridization, which imposes the inter-element normal continuity of the stress by a Lagrange multiplier. Then, we develop and analyze multilevel solvers for the Schur complement of the hybridized system in the two dimensional case. Provided that no nearly singular vertex on the grids, the proposed solvers are proved to be uniformly convergent with respect to both the grid size and Poisson's ratio. Numerical experiments are provided to validate our theoretical results.

Mathematics Subject Classification 65N30 · 65N55

1 Introduction

The mixed finite element methods are popular in solid mechanics since they avoid locking and provide a straightforward approximation for stress. The conforming mixed

✉ Jinchao Xu
xu@math.psu.edu

Shihua Gong
gongshihua@pku.edu.cn

Shuonan Wu
sxw58@psu.edu

¹ Beijing International Center for Mathematical Research, Peking University, Beijing 100871, People's Republic of China

² Department of Mathematics, Pennsylvania State University, University Park, PA 16802, USA

methods based on the classical Hellinger-Reissner variational formulation requires finite element space for the stress in $H(\text{div}; \mathbb{S})$, the space of symmetric matrix-valued fields, which are square integrable with square integrable divergence. In the meantime, the discrete space for the stress must be compatible with that for the displacement, which is a subspace of the vector-valued L^2 space. However, the construction of such stable pairs using polynomial shape functions is very challenging.

To overcome this difficulty, the earliest works adopted composite element techniques (cf. [7,38]). The composite element methods approximate the displacement in one grid while approximating the stress in the refined grid. Due to the difficulties in keeping the symmetry and conformity at the same time, some compromised methods that relax one of the two requirements have been developed. The first category of such methods (cf. [2,8,14,23,29,44,45]) weakly imposes stress symmetry, while maintaining exact $H(\text{div})$ conformity. These methods introduce the Lagrange multiplier, approximating the non-symmetric part of the displacement gradient while enforcing stress symmetry weakly. The second category of such methods (cf. [12,13,33,42,53,55,56]) relaxes the conformity constraints while keeping the symmetry strongly.

In [11], Arnold and Winther proposed the first family of mixed finite element methods in two dimension (2D), which yields the symmetric and conforming approximation for the stress. Since then, many stable mixed elements have been constructed, see [1,4,5]. However, the shape function spaces of these elements, using incomplete polynomials, are quite complicated. In [34,35], Hu and Zhang constructed a family of mixed finite elements with conforming and symmetric stress approximation in a unified fashion on simplex grids for spatial dimension $n = 2, 3$. The degrees of the polynomials to approximate the stress and displacement match reasonably and naturally, by which these elements also achieve the optimal order of convergence. The generalizations or variants of Hu-Zhang's finite elements can be found in [31,32,36].

Both families of the conforming elements above are subject to continuity constraints at the element vertices, which is not natural for $H(\text{div})$ conformity and prohibits techniques like hybridization that are usually available for the mixed method. One feature of our methods is to relax the continuity at the element vertices using the full $C^{\text{div}}-\mathcal{P}_{k+1}$ space for the stress

$$\Sigma_{h,k+1} = \{\boldsymbol{\tau} \in H(\text{div}, \Omega; \mathbb{S}) \mid \boldsymbol{\tau}|_K \in \mathcal{P}_{k+1}(K; \mathbb{S}) \quad \forall K \in \mathcal{T}_h\}.$$

Taking the full $C^{-1}-\mathcal{P}_k$ vector-valued space $V_{h,k}$ for the displacement, the stability of $\Sigma_{h,k+1} - V_{h,k}$ follows directly from the results of [31,34,35] when $k \geq n$. On some special grids, we can still prove the stability for the lower order pairs when $n-2 \leq k < n$. In the 2D case, it is feasible to construct nodal basis functions for $\Sigma_{h,k+1}$ by geometric analysis at the vertices (cf. [43]). In the 3D case, however, it is complicated to deal with nodal basis functions associated with the vertices or edges. In any case, the dimension of $\Sigma_{h,k+1}$ therefore depends on the singular vertices (cf. [43]) or singular edges of the grids.

Instead of constructing basis functions for $\Sigma_{h,k+1}$, we implement it by hybridization (cf. [6,24]). In other words, we remove the inter-element continuity of stress and enforce it by the Lagrange multiplier—the piecewise discontinuous polynomial space

of degree $k + 1$ defined on the edges or faces. The stress and displacement can be eliminated locally in the hybridized mixed system, which results in a linear system solely for the Lagrange multiplier. The resulting multiplier system may have a non-trivial kernel due to the singular vertices or singular edges on the grids but leads to a unique solution of the stress and displacement. Related works on hybridizable methods for elasticity can be found in [27,46,51]. In [27], a family of nonconforming and hybridizable elements on simplicial grids was developed in both 2D and 3D cases. The hybridizable discontinuous Galerkin (HDG) methods for the linear elasticity were studied in [46,51].

Another feature of our methods is to develop robust iterative solvers for the Schur complement of the hybridized mixed system in the 2D case, provided that there is no nearly singular vertex on the grids. The iterative solvers for the hybridized mixed method for the diffusion problem were studied in [22,26,28,40,41]. Although the methodologies in dealing with the non-nested multilevel finite element spaces and the non-inherited bilinear forms were discussed in these papers for the diffusion problem, two essential distinctions exist for the linear elasticity: (i) some local estimates do not hold on each element, but on the element patch, and (ii) the condition number of the multiplier system depends not only on the grid size but also on Poisson's ratio.

To overcome these difficulties, we first establish some local estimates on the element patches by characterizing the inter-element jump of piecewise discontinuous symmetric-matrix-valued polynomials (see Lemmas 7 and 8). We then propose an equivalent norm to the energy norm associated with the multiplier system, which indicates that the multiplier system holds a similar structure with that of the stable discretization (P_2-P_0) for the elastic primal formulation (cf. [47]). Thus, capturing the rigid-body motion mode and the weak divergence-free mode simultaneously is the key to developing robust iterative solvers with respect to both the grid size and Poisson's ratio.

The rest of the paper is organized as follows. In the next section, we introduce our mixed finite element methods and prove their stability and convergence. In Sect. 3, we present the hybridization of the mixed finite element method. We also characterize the kernel of the hybridized mixed system and develop some tools to estimate the norms. In Sect. 4, we focus on the iterative solvers for the multiplier system. We provide some numerical results in Sect. 5 and give some concluding remarks in Sect. 6. Finally, some technical results can be found in the appendixes.

2 Mixed methods

In this paper, we consider the following linear elasticity problem with Dirichlet boundary condition

$$\begin{cases} \mathcal{A}\sigma - \boldsymbol{\epsilon}(u) = 0 & \text{in } \Omega, \\ \operatorname{div}\sigma = f & \text{in } \Omega, \\ u = 0 & \text{on } \partial\Omega, \end{cases} \quad (1)$$

where Ω is a polygonal domain in \mathbb{R}^n ($n = 2, 3$). The displacement and stress are denoted by $u : \Omega \mapsto \mathbb{R}^n$ and $\sigma : \Omega \mapsto \mathbb{S}$, respectively. Here, \mathbb{S} represents the space of

real symmetric matrices of order $n \times n$. The compliance tensor $\mathcal{A} : \mathbb{S} \mapsto \mathbb{S}$ is defined as

$$\mathcal{A}\sigma := \frac{1}{2\tilde{\mu}} \left(\sigma - \frac{\tilde{\lambda}}{2\tilde{\mu} + n\tilde{\lambda}} \text{tr}(\sigma) \mathbf{I} \right), \quad (2)$$

where $\tilde{\mu}, \tilde{\lambda}$ are the Lamé constants. Clearly, \mathcal{A} is bounded and symmetric positive definite. The linearized strain tensor is denoted by $\boldsymbol{\varepsilon}(u) = (\nabla u + (\nabla u)^T)/2$.

2.1 Preliminaries

Let \mathcal{T}_h be a family of quasi-uniform triangulations (cf. [15]) of Ω . Let h_K be the diameter of element $K \in \mathcal{T}_h$, and $h = \max_K h_K$ be the grid diameter of \mathcal{T}_h . For any $K \in \mathcal{T}_h$, the set of all elements that share vertex with K is denoted by ω_K . The sets of all faces and nodes of \mathcal{T}_h are denoted by \mathcal{F}_h and \mathcal{N}_h , respectively. Moreover, \mathcal{F}_h can be divided into two subsets: the boundary faces set $\mathcal{F}_h^\partial = \mathcal{F}_h \cap \partial\Omega$ and the interior faces set $\mathcal{F}_h^i = \mathcal{F}_h \setminus \mathcal{F}_h^\partial$. The unit normal vector with respect to the face F is represented by ν_F .

Let $F \in \mathcal{F}_h^i$ be the common face of two elements K^+ and K^- , and ν_F^+ and ν_F^- be the unit outward normal vectors on F with respect to K^+ and K^- , respectively. Then, we define the jump $[\cdot]$ on $F \in \mathcal{F}_h^i$ for $\boldsymbol{\tau}$ by:

$$[\boldsymbol{\tau}]_F := \boldsymbol{\tau}_{K^+} \nu_F^+ + \boldsymbol{\tau}_{K^-} \nu_F^-.$$

For $F \in \mathcal{F}_h^\partial$, we define $[\boldsymbol{\tau}]_F := \boldsymbol{\tau} \nu$, where ν is the unit outer normal along $\partial\Omega$.

Our notation for the inner products is standard (cf. [15]): For $u, v \in L^2(D)$, we write $(u, v)_D = \int_D uv \, dx$ if D is a subdomain of \mathbb{R}^n , and $\langle u, v \rangle_D = \int_D uv \, ds$ if D is a subdomain of \mathbb{R}^{n-1} . We neglect the subscript D if $D = \Omega$. To emphasize the mesh-dependent nature of certain integrals, for $\tilde{\mathcal{T}}_h \subset \mathcal{T}_h$ and $\tilde{\mathcal{F}}_h \subset \mathcal{F}_h$, we define

$$(u_h, v_h)_{\tilde{\mathcal{T}}_h} := \sum_{K \in \tilde{\mathcal{T}}_h} (u_h, v_h)_K \quad \text{and} \quad \langle \lambda_h, \mu_h \rangle_{\tilde{\mathcal{F}}_h} := \sum_{F \in \tilde{\mathcal{F}}_h} \langle \lambda_h, \mu_h \rangle_F,$$

where u_h, v_h and μ_h, λ_h are defined on $\tilde{\mathcal{T}}_h$ and $\tilde{\mathcal{F}}_h$, respectively.

Throughout this paper, we shall use letter C to denote a generic positive constant independent of h and the material parameters. Note that C may stand for different values at its various occurrences. The notation $x \lesssim y$ means $x \leq Cy$ and $x \simeq y$ means $x \lesssim y \lesssim x$.

The mixed formulation of (1) is to find $(\sigma, u) \in \Sigma \times V := H(\text{div}, \Omega; \mathbb{S}) \times L^2(\Omega; \mathbb{R}^n)$ such that

$$\begin{cases} (\mathcal{A}\sigma, \boldsymbol{\tau}) + (\text{div}\boldsymbol{\tau}, u) = 0 & \forall \boldsymbol{\tau} \in \Sigma, \\ (\text{div}\sigma, v) = (f, v) & \forall v \in V. \end{cases} \quad (3)$$

Here, $H(\text{div}, \Omega; \mathbb{S})$ consists of square-integrable symmetric matrix fields with square-integrable divergence, and $L^2(\Omega; \mathbb{R}^n)$ is the space of vector-valued functions that are square integrable with the standard L^2 norm. The corresponding $H(\text{div})$ norm is defined by

$$\|\boldsymbol{\tau}\|_{H(\text{div})}^2 := \|\boldsymbol{\tau}\|_0^2 + \|\text{div} \boldsymbol{\tau}\|_0^2 \quad \forall \boldsymbol{\tau} \in H(\text{div}, \Omega; \mathbb{S}).$$

We take the discrete stress space as the full $C^{\text{div}}-\mathcal{P}_{k+1}$ space

$$\Sigma_{h,k+1} := \{\boldsymbol{\tau} \in H(\text{div}, \Omega; \mathbb{S}) \mid \boldsymbol{\tau}|_K \in \mathcal{P}_{k+1}(K; \mathbb{S}) \quad \forall K \in \mathcal{T}_h\}, \quad (4)$$

and take the discrete displacement space as the full $C^{-1}-\mathcal{P}_k$ space

$$V_{h,k} := \{v \in L^2(\Omega; \mathbb{R}^n) \mid v|_K \in \mathcal{P}_k(K, \mathbb{R}^n) \quad \forall K \in \mathcal{T}_h\}. \quad (5)$$

Then, the mixed finite element approximation of the elastic problem (3) reads: Find $(\boldsymbol{\sigma}_h, u_h) \in \Sigma_{h,k+1} \times V_{h,k}$ such that

$$\begin{cases} (\mathcal{A}\boldsymbol{\sigma}_h, \boldsymbol{\tau}_h) + (u_h, \text{div} \boldsymbol{\tau}_h) = 0 & \forall \boldsymbol{\tau}_h \in \Sigma_{h,k+1}, \\ (\text{div} \boldsymbol{\sigma}_h, v_h) = (f, v_h) & \forall v_h \in V_{h,k}. \end{cases} \quad (6)$$

2.2 Stability and convergence

The convergence of the finite element solution follows from the stability and the standard approximation property. First, we consider the stability of the discrete problem (6), which follows from two conditions by the standard theory of mixed finite element methods (cf. [18]).

1. K-ellipticity: There exists a constant $\alpha > 0$, independent of the grid size, such that

$$(\mathcal{A}\boldsymbol{\tau}_h, \boldsymbol{\tau}_h) \geq \alpha \|\boldsymbol{\tau}_h\|_{H(\text{div})}^2 \quad \forall \boldsymbol{\tau}_h \in Z_h, \quad (7)$$

where $Z_h := \{\boldsymbol{\tau}_h \in \Sigma_{h,k+1} \mid (\text{div} \boldsymbol{\tau}_h, v_h) = 0 \quad \forall v_h \in V_{h,k}\} = \{\boldsymbol{\tau}_h \in \Sigma_{h,k+1} \mid \text{div} \boldsymbol{\tau}_h = 0\}$.

2. Ladyženskaja-Babuška-Brezzi (LBB) condition: There exists a constant $\beta > 0$, independent of the grid size, such that

$$\inf_{v_h \in V_h} \sup_{\boldsymbol{\tau}_h \in \Sigma_{h,k+1}} \frac{(\text{div} \boldsymbol{\tau}_h, v_h)}{\|\boldsymbol{\tau}_h\|_{H(\text{div})} \|v_h\|_0} \geq \beta. \quad (8)$$

Since $\text{div} \Sigma_{h,k+1} \subset V_{h,k}$ for any $k \geq 0$, we know that $Z_h \in \ker(\text{div})$. Therefore,

$$(\mathcal{A}\boldsymbol{\tau}_h, \boldsymbol{\tau}_h) \geq C \|\boldsymbol{\tau}_h\|_0^2 = C \|\boldsymbol{\tau}_h\|_{H(\text{div})}^2 \quad \forall \boldsymbol{\tau}_h \in Z_h, \quad (9)$$

as the compliance tensor is positive definite. This implies the K-ellipticity. Note that, pertaining to $\int_{\Omega} \text{tr}(\boldsymbol{\tau}_h) dx = 0$, the constant C in (9) is uniform with respect to the Poisson's ratio ($\tilde{\nu} := \frac{\tilde{\lambda}}{2(\tilde{\lambda} + \tilde{\mu})}$) due to the following theorem (see Sect. 9 in [18] for details).

Theorem 1 *Assume that $\boldsymbol{\sigma} \in H(\text{div}, \Omega; \mathbb{S})$ satisfies $\int_{\Omega} \text{tr}(\boldsymbol{\sigma}) = 0$ and $\text{div} \boldsymbol{\sigma} = 0$. It holds that*

$$\|\boldsymbol{\sigma}\|_0^2 \lesssim 2\tilde{\mu}(\mathcal{A}\boldsymbol{\sigma}, \boldsymbol{\sigma}). \quad (10)$$

Next, we discuss the inf-sup condition under the pure displacement boundary condition. Similar techniques work for the traction boundary condition.

Lemma 1 *When $k \geq n$, for any $v_h \in V_{h,k}$, there exists $\boldsymbol{\tau}_h \in \Sigma_{h,k+1}$ such that*

$$\text{div} \boldsymbol{\tau}_h = v_h \quad \text{and} \quad \|\boldsymbol{\tau}_h\|_{H(\text{div})} \lesssim \|v_h\|_0. \quad (11)$$

Proof This is a corollary of [31, 34, 35], in which a family of finite elements for $H(\text{div}, \Omega; \mathbb{S})$ satisfying (11) is proposed as

$$\begin{aligned} \Sigma_{h,k+1}^{\text{HZ}} := \{&\boldsymbol{\tau} \in H(\text{div}, \Omega; \mathbb{S}) \mid \boldsymbol{\tau} = \boldsymbol{\tau}_c + \boldsymbol{\tau}_b, \boldsymbol{\tau}_c \in H^1(\Omega; \mathbb{S}), \\ &\boldsymbol{\tau}_c|_K \in \mathcal{P}_{k+1}(K; \mathbb{S}), \boldsymbol{\tau}_b|_K \in \Sigma_{k+1,b}(K) \quad \forall K \in \mathcal{T}_h\}. \end{aligned} \quad (12)$$

Here, the local conforming div-bubble space $\Sigma_{k+1,b}(K) := \{\boldsymbol{\tau} \in \mathcal{P}_{k+1}(K; \mathbb{S}) \mid \boldsymbol{\tau} v|_{\partial K} = 0\}$. Hence, the lemma follows from the fact that $\boldsymbol{\tau}_h \in \Sigma_{h,k+1}^{\text{HZ}} \subset \Sigma_{h,k+1}$. \square

For the lower order case, the inf-sup condition (11) resorts to some known results of the Stokes pair. When $k \geq n - 2$, the Stokes pair $\mathcal{P}_{k+2} - \mathcal{P}_{k+1}^{-1}$ can be proved stable on special grids (cf. [10, 57]), a popular example of which is the Hsieh-Clough-Tocher (HCT) grid, where each macro-simplex is divided into $n + 1$ sub-simplexes by connecting the barycenter with the vertices.

Lemma 2 *When $n - 2 \leq k < n$, if the Stokes pair $\mathcal{P}_{k+2} - \mathcal{P}_{k+1}^{-1}$ is stable on the grid, then for any $v_h \in V_{h,k}$, there exists $\boldsymbol{\tau}_h \in \Sigma_{h,k+1}$ such that*

$$\text{div} \boldsymbol{\tau}_h = v_h \quad \text{and} \quad \|\boldsymbol{\tau}_h\|_{H(\text{div})} \lesssim \|v_h\|_0. \quad (13)$$

Proof We prove the stability by a constructive method (cf. [8]). In light of the Brezzi-Douglas-Marini (BDM) elements for $H(\text{div}; \mathbb{R}^n)$ (cf. [17, 18]), we defined the following space

$$\text{BDM}_{k+1}^{n \times n} := \{\boldsymbol{\tau} \in H(\text{div}, \Omega; \mathbb{M}) \mid \boldsymbol{\tau}|_K \in \mathcal{P}_{k+1}(K; \mathbb{M}) \quad \forall K \in \mathcal{T}_h\},$$

where \mathbb{M} represents the space of real matrices of order $n \times n$. The $\text{div} \boldsymbol{\tau}$ here is defined by taking div on each row of $\boldsymbol{\tau}$. By the stability of BDM elements, we immediately know that for any $v_h \in V_h$, there exists a $\tilde{\boldsymbol{\tau}}_h \in \text{BDM}_{k+1}^{n \times n}$ such that

$$\text{div} \tilde{\boldsymbol{\tau}}_h = v_h \quad \text{and} \quad \|\tilde{\boldsymbol{\tau}}_h\|_{H(\text{div})} \lesssim \|v_h\|_0.$$

With the purpose of symmetrizing $\boldsymbol{\tau}_h$, we add a divergence-free term to $\tilde{\boldsymbol{\tau}}_h$ to obtain

$$\boldsymbol{\tau}_h = \tilde{\boldsymbol{\tau}}_h + \operatorname{curl} \rho_h,$$

where ρ_h satisfies

1. For $n = 2$: $\rho_h \in H^1(\Omega; \mathbb{R}^2)$ is a vector-valued function and $\rho_h|_K \in \mathcal{P}_{k+2}(K; \mathbb{R}^2)$;
2. For $n = 3$: $\rho_h \in H^1(\Omega; \mathbb{M})$ is a matrix-valued function and $\rho_h|_K \in \mathcal{P}_{k+2}(K; \mathbb{M})$.

For the 2D case, the curl operator is a rotation of the operator ∇ (i.e., $\operatorname{curl} = (-\partial_y, \partial_x)$) and applies on each entry of the vector ρ_h . For the 3D case, the curl operator applies on each row of the matrix ρ_h . By direct calculation, the symmetry of $\boldsymbol{\tau}_h$ is equivalent to the following equation,

$$\operatorname{skw}(\operatorname{curl} \rho_h) = -\operatorname{skw} \tilde{\boldsymbol{\tau}}_h, \quad (14)$$

where $\operatorname{skw} \boldsymbol{\tau} := (\boldsymbol{\tau} - \boldsymbol{\tau}^T)/2$. For a scalar function v and a vector-valued function $v = (v_1, v_2, v_3)^T$, we further define

$$\operatorname{Skw}_2(v) := \begin{bmatrix} 0 & v \\ -v & 0 \end{bmatrix} \quad \text{and} \quad \operatorname{Skw}_3(v) := \begin{bmatrix} 0 & v_3 & -v_2 \\ -v_3 & 0 & v_1 \\ v_2 & -v_1 & 0 \end{bmatrix}.$$

Then, the proof can be divided into the following two cases:

1. For $n = 2$: From [9], we have $\operatorname{skw}(\operatorname{curl} \rho_h) = \frac{1}{2} \operatorname{Skw}_2(\operatorname{div} \rho_h)$. Thus, (14) can be written as:

$$\operatorname{div} \rho_h = \tilde{\boldsymbol{\tau}}_{h,21} - \tilde{\boldsymbol{\tau}}_{h,12}. \quad (15)$$

The stability of Stokes pair $\mathcal{P}_{k+2} - \mathcal{P}_{k+1}^{-1}$ then implies that there exists a $\rho_h \in \{v \in H^1(\Omega; \mathbb{R}^2) \mid v|_K \in \mathcal{P}_{k+2}(K; \mathbb{R}^2)\}$ satisfying (15) and

$$\|\rho_h\|_1 \lesssim \|\tilde{\boldsymbol{\tau}}_{h,21} - \tilde{\boldsymbol{\tau}}_{h,12}\|_0 \leq \|\tilde{\boldsymbol{\tau}}_h\|_0 \lesssim \|v_h\|_0.$$

2. For $n = 3$: From [9], we have $\operatorname{skw}(\operatorname{curl} \rho_h) = -\frac{1}{2} \operatorname{Skw}_3(\operatorname{div} \mathcal{E} \rho_h)$, where \mathcal{E} is an algebraic operator defined as $\mathcal{E} \rho_h = \rho_h^T - \operatorname{tr}(\rho_h) \mathbf{I}$. Denoting $\eta_h = \mathcal{E} \rho_h$, it is obvious that $\rho_h = \mathcal{E}^{-1} \eta_h = \eta_h^T - \frac{1}{2} \operatorname{tr}(\eta_h) \mathbf{I}$. Thus, (14) can be written as:

$$\operatorname{div} \eta_h = (\tilde{\boldsymbol{\tau}}_{h,23} - \tilde{\boldsymbol{\tau}}_{h,32}, \tilde{\boldsymbol{\tau}}_{h,31} - \tilde{\boldsymbol{\tau}}_{h,13}, \tilde{\boldsymbol{\tau}}_{h,12} - \tilde{\boldsymbol{\tau}}_{h,21})^T. \quad (16)$$

Again, there exists a $\eta_h \in \{\boldsymbol{\tau} \in H^1(\Omega; \mathbb{M}) \mid \boldsymbol{\tau}|_K \in \mathcal{P}_{k+2}(K; \mathbb{M})\}$ satisfying (16) and

$$\|\rho_h\|_1 \lesssim \|\eta_h\|_1 \lesssim \|\tilde{\boldsymbol{\tau}}_h\|_0 \lesssim \|v_h\|_0.$$

To summarize, we obtain $\boldsymbol{\tau}_h = \tilde{\boldsymbol{\tau}}_h + \operatorname{curl} \rho_h$ that satisfying $\boldsymbol{\tau}_h \in \Sigma_{h,k+1}$,

$$\operatorname{div} \boldsymbol{\tau}_h = v_h \quad \text{and} \quad \|\boldsymbol{\tau}_h\|_{H(\operatorname{div})} \lesssim \|\tilde{\boldsymbol{\tau}}_h\|_{H(\operatorname{div})} + \|\operatorname{curl} \rho_h\|_0 \lesssim \|v_h\|_0.$$

This completes the proof. \square

By virtue of Lemmas 1 and 2, we have the following theorems.

Theorem 2 *Under the conditions in Lemmas 1 or 2, the K-ellipticity (7) and the inf-sup condition (8) hold uniformly with respect to the mesh size. Consequently, the discrete mixed problem (6) is well-posed.*

Theorem 3 *Let $(\boldsymbol{\sigma}, u) \in \Sigma \times V$ be the exact solution of the problem (3) and $(\boldsymbol{\sigma}_h, u_h) \in \Sigma_{h,k+1} \times V_{h,k}$ the finite element solution of (6). Assume that $\boldsymbol{\sigma} \in H^{k+2}(\Omega; \mathbb{S})$ and $u \in H^{k+1}(\Omega; \mathbb{R}^n)$. Under the conditions in Lemmas 1 or 2, we have*

$$\|\boldsymbol{\sigma} - \boldsymbol{\sigma}_h\|_{H(\operatorname{div})} + \|u - u_h\|_0 \lesssim h^{k+1}(|\boldsymbol{\sigma}|_{k+2} + |u|_{k+1}). \quad (17)$$

Proof The well-posedness implies the following quasi-optimal error estimate,

$$\|\boldsymbol{\sigma} - \boldsymbol{\sigma}_h\|_{H(\operatorname{div})} + \|u - u_h\|_0 \lesssim \inf_{\boldsymbol{\tau}_h \in \Sigma_{h,k+1}, v_h \in V_{h,k}} (\|\boldsymbol{\sigma} - \boldsymbol{\tau}_h\|_{H(\operatorname{div})} + \|u - v_h\|_0), \quad (18)$$

which gives rise to (17) due to the standard L^2 projection and Scott-Zhang interpolation (cf. [50]). \square

3 Hybridization

To implement the mixed method (6), we need the degrees of freedom (d.o.f.) or the nodal basis of the discrete stress spaces. In the definition (4), however, we state the inter-element continuity directly instead of using the d.o.f., which is different from Ciarlet's convention for the finite elements. More precisely, there is no locally defined d.o.f. on elements for the discrete stress spaces (4). A similar argument can be found in [11]. In light of [43], where the authors constructed the nodal basis for the space of piecewise C^1 polynomials, we can globally form the nodal basis for our discrete stress spaces, whose dimensions depend on the singular vertices of the grids.

Instead of presenting the details of the nodal basis, we adopt a simpler implementation technique—the hybridization method (cf. [6, 24]), which imposes the inter-element continuity by Lagrange multiplier. The hybridization method removes the inter-element continuity from the space $\Sigma_{h,k+1}$, which results in a discontinuous stress space

$$\Sigma_{h,k+1}^{-1} := \{\boldsymbol{\tau}_h \in L^2(\Omega; \mathbb{S}) \mid \boldsymbol{\tau}_h|_K \in \mathcal{P}_{k+1}(K; \mathbb{S}) \quad \forall K \in \mathcal{T}_h\}. \quad (19)$$

To enforce the inter-element continuity of the stress, we introduce the Lagrange multiplier space $M_{h,k+1}$, where

$$M_{h,k+1} := \{\mu_h \in L^2(\mathcal{F}_h, \mathbb{R}^n) \mid \mu_h|_F \in \mathcal{P}_{k+1}(F, \mathbb{R}^n) \quad \forall F \in \mathcal{F}_h^i, \text{ and } \mu_h|_{\mathcal{F}_h^\partial} = 0\}. \quad (20)$$

The hybridized mixed finite element method is to find $(\sigma_h, u_h, \lambda_h) \in \Sigma_{h,k+1}^{-1} \times V_{h,k} \times M_{h,k+1}$ satisfying

$$(\mathcal{A}\sigma_h, \tau_h)_{\mathcal{T}_h} + (\operatorname{div}_h \tau_h, u_h)_{\mathcal{T}_h} - \langle [\tau_h], \lambda_h \rangle_{\mathcal{F}_h^i} = 0 \quad \forall \tau_h \in \Sigma_{h,k+1}^{-1}, \quad (21a)$$

$$(\operatorname{div}_h \sigma_h, v_h)_{\mathcal{T}_h} = (f, v_h) \quad \forall v_h \in V_{h,k}, \quad (21b)$$

$$-\langle [\sigma_h], \mu_h \rangle_{\mathcal{F}_h^i} = 0 \quad \forall \mu_h \in M_{h,k+1}. \quad (21c)$$

Here, div_h is the broken divergence operator. For convenience, let $\mathcal{B} := \operatorname{div}_h : \Sigma_{h,k+1}^{-1} \mapsto V_{h,k}$ and $\mathcal{C} : \Sigma_{h,k+1}^{-1} \mapsto M_{h,k+1}$ defined by

$$\mathcal{C}\tau|_F := \begin{cases} [\tau]|_F & \text{for } F \in \mathcal{F}_h^i, \\ 0 & \text{for } F \in \mathcal{F}_h^\partial. \end{cases} \quad (22)$$

The adjoint of these operators are defined as $\mathcal{B}^* : V_{h,k} \mapsto \Sigma_{h,k+1}^{-1}$ and $\mathcal{C}^* : M_{h,k+1} \mapsto \Sigma_{h,k+1}^{-1}$ such that for any $(\tau_h, v_h, \mu_h) \in \Sigma_{h,k+1}^{-1} \times V_{h,k} \times M_{h,k+1}$,

$$(\mathcal{B}^*v_h, \tau_h) = (v_h, \mathcal{B}\tau_h) \quad \text{and} \quad (\mathcal{C}^*\mu_h, \tau_h) = \langle \mu_h, \mathcal{C}\tau_h \rangle_{\mathcal{F}_h^i}.$$

The following theorem shows the property of hybridized method given in (21).

Theorem 4 *There exists a solution $(\sigma_h, u_h, \lambda_h) \in \Sigma_{h,k+1}^{-1} \times V_{h,k} \times M_{h,k+1}$ for the hybridized system (21). Moreover, the first two components of the solution are unique and coincide with that of the mixed method (6).*

Proof By Theorem 2, there exists a solution $(\sigma_h, u_h) \in \Sigma_{h,k+1} \times V_{h,k}$ for the mixed method (6). It is obvious that (σ_h, u_h) satisfies the last two equations (21b) and (21c). The first equation (21a) can be written as

$$\mathcal{C}^*\lambda_h = \mathcal{A}\sigma_h + \mathcal{B}^*u_h. \quad (23)$$

Since $R(\mathcal{C}^*)^\perp = \ker(\mathcal{C})$ and $\ker(\mathcal{C}) = \Sigma_{h,k+1}$, we have

$$R(\mathcal{C}^*) = (\Sigma_{h,k+1})^\perp.$$

Here, $(\Sigma_{h,k+1})^\perp$ is the L^2 orthogonal complement of $\Sigma_{h,k+1}$ in $\Sigma_{h,k+1}^{-1}$ with respect to the inner product (\cdot, \cdot) . Since (σ_h, u_h) satisfies (21a) for $\tau_h \in \Sigma_{h,k+1}$, it holds that

$$\mathcal{A}\sigma_h + \mathcal{B}^*u_h \in (\Sigma_{h,k+1})^\perp. \quad (24)$$

Hence, there exists $\lambda_h \in M_{h,k+1}$ satisfying (23), which indicates the existence of the solution for (21).

Table 1 $\tilde{\Sigma}_{h,k+n-}$, $\Sigma_{h,k+1}^{\text{HZ}}$ and their hybridized versions

Elements	Gerneral grids	Special grids	Hybridizable	Lagrange multiplier
$\tilde{\Sigma}_{h,k+n-} - V_{h,k}$	$k \geq 1$	—	×	—
$\Sigma_{h,k+1}^{\text{HZ}} - V_{h,k}$	$k \geq n$	—	×	—
$\Sigma_{h,k+n-} - V_{h,k}$	$k \geq 1$	—	✓	$M_{h,k+n}$
$\Sigma_{h,k+1} - V_{h,k}$	$k \geq n$	$k \geq n-2$	✓	$M_{h,k+1}$

For the uniqueness, assuming that $(\sigma_h, u_h, \lambda_h)$ satisfies (21), then (21c) implies that $\sigma_h \in \Sigma_{h,k+1}$. Moreover, since $\Sigma_{h,k+1} \subset \Sigma_{h,k+1}^{-1}$, choosing $\tau_h \in \Sigma_{h,k+1}$, we can see that the system (21a) and (21b) is identical to the system of the mixed method (6). Therefore, (σ_h, u_h) solves (6). The uniqueness of (σ_h, u_h) follows from Theorem 2. This completes the proof. \square

Remark 1 We note that Hu-Zhang elements in (12) can also be written as

$$\Sigma_{h,k+1}^{\text{HZ}} = \{\boldsymbol{\tau} \in H(\text{div}, \Omega; \mathbb{S}) \mid \boldsymbol{\tau}|_K \in \mathcal{P}_{k+1}(K; \mathbb{S}) \quad \forall K \in \mathcal{T}_h, \\ \text{and } \boldsymbol{\tau}|_a \text{ is continuous for any } a \in \mathcal{N}_h\}.$$

We enrich the space $\Sigma_{h,k+1}^{\text{HZ}}$ by relaxing the continuity on the element vertices. Similar technique can be used in Arnold-Winther [11] ($n = 2$) or Arnold-Awanou-Winther [5] ($n = 3$) elements $\tilde{\Sigma}_{h,k+n-} - V_{h,k}$, where

$$\tilde{\Sigma}_{h,k+n-} := \{\boldsymbol{\tau} \in H(\text{div}, \Omega; \mathbb{S}) \mid \boldsymbol{\tau}|_K \in \tilde{\Sigma}_{k+n-}(K) \quad \forall K \in \mathcal{T}_h, \\ \text{and } \boldsymbol{\tau}|_a \text{ is continuous for any } a \in \mathcal{N}_h\}.$$

and $\tilde{\Sigma}_{k+n-}(K) := \{\boldsymbol{\tau} \in \mathcal{P}_{k+n}(K; \mathbb{S}) \mid \text{div} \boldsymbol{\tau} \in \mathcal{P}_k(K; \mathbb{R}^n)\}$. We denote the hybridized version of $\tilde{\Sigma}_{h,k+n-}$ by

$$\Sigma_{h,k+n-} := \{\boldsymbol{\tau} \in H(\text{div}, \Omega; \mathbb{S}) \mid \boldsymbol{\tau}|_K \in \tilde{\Sigma}_{k+n-}(K) \quad \forall K \in \mathcal{T}_h\}.$$

Table 1 compares $\tilde{\Sigma}_{h,k+n-}$ and $\Sigma_{h,k+1}^{\text{HZ}}$ to their hybridized versions.

3.1 SPD system for lagrange multiplier

Theorem 4 implies that the kernel of the hybridized mixed system (21) is $\{0\} \times \{0\} \times \ker(\mathcal{C}^*)$. It is straightforward that $\ker(\mathcal{C}^*) = R(\mathcal{C})^\perp$, where $R(\mathcal{C})^\perp$ is the L^2 orthogonal complement of $R(\mathcal{C})$ in the space $M_{h,k+1}$ with respect to the inner product $\langle \cdot, \cdot \rangle_{\mathcal{F}_h^i}$. We therefore have the following decomposition for the multiplier space

$$M_{h,k+1} = R(\mathcal{C}) \oplus R(\mathcal{C})^\perp.$$

We note that the dimension of $R(\mathcal{C})^\perp$ depends on the grid.

Lemma 3 Both $\mathbf{R}(\mathcal{C})$ and $\mathbf{R}(\mathcal{C})^\perp$ have local bases, that is,

$$\begin{aligned}\mathbf{R}(\mathcal{C}) &= \text{span}\{\varphi_1, \varphi_2, \dots, \varphi_{N_1}\}, \\ \mathbf{R}(\mathcal{C})^\perp &= \text{span}\{\psi_1, \psi_2, \dots, \psi_{N_2}\},\end{aligned}$$

where $\varphi_i, \psi_j \in M_{h,k+1}$ are locally supported and N_1, N_2 are the dimensions of the spaces $\mathbf{R}(\mathcal{C}), \mathbf{R}(\mathcal{C})^\perp$, respectively.

Proof We construct the Lagrange-type bases of $\mathbf{R}(\mathcal{C})$ and $\mathbf{R}(\mathcal{C})^\perp$ in Appendix A. \square

We eliminate the variables $\boldsymbol{\sigma}_h$ and u_h in the hybridized mixed system (21), then obtain a linear system solely for λ_h . For any $\lambda \in M_{h,k+1}$, we define two local problems:

1. Find $(\boldsymbol{\sigma}_\lambda, u_\lambda) \in \Sigma_{h,k+1}^{-1} \times V_{h,k}$ such that for any element $K \in \mathcal{T}_h$,

$$(\mathcal{A}\boldsymbol{\sigma}_\lambda, \boldsymbol{\tau}_h)_K + (u_\lambda, \text{div}\boldsymbol{\tau}_h)_K = \langle \lambda, \boldsymbol{\tau}_h v \rangle_{\partial K} \quad \forall \boldsymbol{\tau}_h \in \mathcal{P}_{k+1}(K; \mathbb{S}), \quad (25a)$$

$$(\text{div}\boldsymbol{\sigma}_\lambda, v_h)_K = 0 \quad \forall v_h \in \mathcal{P}_k(K; \mathbb{R}^n). \quad (25b)$$

2. Find $(\tilde{\boldsymbol{\sigma}}_f, \tilde{u}_f) \in \Sigma_{h,k+1}^{-1} \times V_{h,k}$ such that for any element $K \in \mathcal{T}_h$,

$$(\mathcal{A}\tilde{\boldsymbol{\sigma}}_f, \boldsymbol{\tau}_h)_K + (\tilde{u}_f, \text{div}\boldsymbol{\tau}_h)_K = 0 \quad \forall \boldsymbol{\tau}_h \in \mathcal{P}_{k+1}(K; \mathbb{S}), \quad (26a)$$

$$(\text{div}\tilde{\boldsymbol{\sigma}}_f, v_h)_K = (f, v_h)_K \quad \forall v_h \in \mathcal{P}_k(K; \mathbb{R}^n). \quad (26b)$$

The following lemma shows that both $(\boldsymbol{\sigma}_m, u_m)$ and $(\tilde{\boldsymbol{\sigma}}_f, \tilde{u}_f)$ are well defined.

Lemma 4 The systems (25) and (26) are unisolvant. Moreover, the solution of the system (21) satisfies

$$\boldsymbol{\sigma}_h = \boldsymbol{\sigma}_{\lambda_h} + \tilde{\boldsymbol{\sigma}}_f \quad \text{and} \quad u_h = u_{\lambda_h} + \tilde{u}_f. \quad (27)$$

Proof The proof is similar to the standard one given in [24] and is therefore omitted here. \square

Note that $(\boldsymbol{\sigma}_{\lambda_h}, u_{\lambda_h})$ and $(\tilde{\boldsymbol{\sigma}}_f, \tilde{u}_f)$ can be computed element by element. The above lemma means that the $\boldsymbol{\sigma}_h$ and u_h can be locally recovered after solving the variable λ_h .

Theorem 5 The Lagrange multiplier λ_h satisfies

$$s(\lambda_h, \mu_h) = -(f, u_{\mu_h}) \quad \forall \mu \in M_{h,k+1}, \quad (28)$$

where $s(\lambda_h, \mu_h) = (\mathcal{A}\boldsymbol{\sigma}_{\lambda_h}, \boldsymbol{\sigma}_{\mu_h})$. Moreover, the system (28) is symmetric positive-semidefinite and its kernel is $\mathbf{R}(\mathcal{C})^\perp$. Namely, the system (28) is symmetric positive-definite in $\mathbf{R}(\mathcal{C})$.

Proof The derivation of (28) is standard in the hybridization method (cf. [24]). The kernel of the multiplier system is the same with the hybridized mixed system. \square

Remark 2 The feasibility of the hybridization technique relies on the solvability of the local systems (25) and (26) and the solvability of global system of the Lagrange multiplier. Lemma 4 indicates the well-posedness of the local systems. For the global system (28), one can show the consistence of the right hand side by

$$-(f, u_{\mu_h}) = 0 \quad \forall \mu_h \in R(C)^\perp,$$

since $R(S) = R(C)$ and $u_{\mu_h} = 0, \forall \mu_h \in R(C)^\perp$. Thus, by Theorem 5, there exists a unique solution of (28) on $R(C)$. Actually, by using the Krylov subspace solvers, the numerical solution of Lagrange multiplier in (28) can be approximated with a pre-chosen tolerance. Since the local problems (25) and (26) are well-posedness, we can numerically recover the stress and the displacement in a satisfying accuracy. Thus, the semidefiniteness of the global system does not stain the hybridization process.

3.2 Norm estimates

We denote the linear operator corresponding to the bilinear form $s(\cdot, \cdot)$ by $\mathcal{S} : M_{h,k+1} \mapsto M_{h,k+1}$, or $S : M_{h,k+1} \mapsto M'_{h,k+1}$ as

$$\langle S\lambda, \mu \rangle := \langle \mathcal{S}\lambda, \mu \rangle_{\mathcal{F}_h^i} := s(\lambda, \mu) \quad \forall \lambda, \mu \in M_{h,k+1}. \quad (29)$$

In fact, \mathcal{S} is the Schur complement of the hybridized mixed system (21). In light of Theorem 5, we can define a norm $\|\cdot\|_S$ on $R(C)$ as

$$\|\lambda\|_S^2 := \sum_{K \in \mathcal{T}_h} \|\lambda\|_{S,K}^2 := \sum_{K \in \mathcal{T}_h} (\mathcal{A}\sigma_\lambda, \sigma_\lambda)_K \quad \forall \lambda \in R(C), \quad (30)$$

which can also be extended as a semi-norm on $M_{h,k+1}$. For the conciseness, we still denote the semi-norm on $M_{h,k+1}$ by $\|\cdot\|_S$.

To investigate how $\|\cdot\|_S$ depends on the parameters, we define the following semi-norms locally:

$$|\lambda|_{h,K} := \sup_{\tau \in Z_h(K)} \frac{\langle \lambda, \tau v \rangle_{\partial K}}{\|\tau\|_{0,K}} \quad \forall \lambda \in M_{h,k+1}, \quad (31)$$

$$|\lambda|_{*,K} := |K|^{-1/2} \left| \int_{\partial K} \lambda \cdot v \, ds \right| \quad \forall \lambda \in M_{h,k+1}. \quad (32)$$

Here, $Z_h(K) = \{\tau_h \in \mathcal{P}_{k+1}(K; \mathbb{S}) \mid \text{div} \tau_h = 0\}$. The semi-norms $|\cdot|_h$ and $|\cdot|_*$ on $M_{h,k+1}$ are defined by the summations of local norms over all elements, namely,

$$|\lambda|_h^2 = \sum_{K \in \mathcal{T}_h} |\lambda|_{h,K}^2 \quad \text{and} \quad |\lambda|_*^2 = \sum_{K \in \mathcal{T}_h} |\lambda|_{*,K}^2.$$

The relationship between $\|\cdot\|_S$ and $|\cdot|_*, |\cdot|_h$ is described in the following lemma.

Theorem 6 *It holds that*

$$\|\lambda\|_{S,K}^2 \approx 2\tilde{\mu}|\lambda|_{h,K}^2 + \tilde{\lambda}|\lambda|_{*,K}^2 \quad \forall \lambda \in M_{h,k+1}. \quad (33)$$

Proof Notice that $\sigma_\lambda|_K \in Z_h(K)$ by (25b). Moreover, for any $\tau \in Z_h(K)$, by (25a), we have

$$(\mathcal{A}\sigma_\lambda, \tau)_K = \langle \lambda, \tau v \rangle_{\partial K}. \quad (34)$$

Let $m_\tau = \frac{1}{n|K|} \int_K \text{tr}(\tau) dx$ and $\tau_0 = \tau - m_\tau \mathbf{I}$. Then $(\tau_0, \mathbf{I})_K = 0$ and $(\mathcal{A}\tau_0, \mathbf{I})_K = 0$, which implies that

$$(\mathcal{A}\tau, \tau)_K = (\mathcal{A}\tau_0, \tau_0)_K + (\mathcal{A}m_\tau \mathbf{I}, m_\tau \mathbf{I})_K.$$

Let $\|\tau\|_{\mathcal{A},K} := (\mathcal{A}\tau, \tau)_K^{1/2}$ for any $\tau \in L^2(K; \mathbb{S})$. In light of (10) and (34), we have for any $\lambda \in M_{h,k+1}$,

$$\begin{aligned} \|\lambda\|_{S,K} &= \sup_{\tau \in Z_h(K)} \frac{(\mathcal{A}\sigma_\lambda, \tau)_K}{\|\tau\|_{\mathcal{A},K}} = \sup_{\tau \in Z_h(K)} \frac{\langle \lambda, \tau v \rangle_{\partial K}}{\|\tau\|_{\mathcal{A},K}} \\ &\leq \sup_{\tau \in Z_h(K)} \frac{\langle \lambda, \tau_0 v \rangle_{\partial K}}{\|\tau\|_{\mathcal{A},K}} + \sup_{\tau \in Z_h(K)} \frac{\langle \lambda, m_\tau \mathbf{I} v \rangle_{\partial K}}{\|\tau\|_{\mathcal{A},K}} \\ &= \sup_{\tau \in Z_h(K)} \frac{\langle \lambda, \tau_0 v \rangle_{\partial K}}{\|\tau_0\|_{\mathcal{A},K}} + \sup_{\tau \in Z_h(K)} \frac{\langle \lambda, m_\tau \mathbf{I} v \rangle_{\partial K}}{\|m_\tau \mathbf{I}\|_{\mathcal{A},K}} \\ &\lesssim (2\tilde{\mu})^{1/2} \sup_{\tau \in Z_h(K)} \frac{\langle \lambda, \tau_0 v \rangle_{\partial K}}{\|\tau_0\|_{0,K}} + \tilde{\lambda}^{1/2} |\lambda|_{*,K} \\ &\lesssim (2\tilde{\mu})^{1/2} |\lambda|_{h,K} + \tilde{\lambda}^{1/2} |\lambda|_{*,K}. \end{aligned}$$

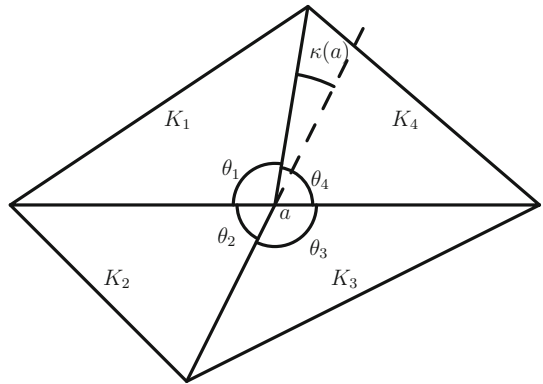
On the other hand, since $2\tilde{\mu}(\mathcal{A}\tau, \tau)_K \lesssim \|\tau\|_{0,K}^2$ by the definition of \mathcal{A} , we have

$$(2\tilde{\mu})^{1/2} |\lambda|_{h,K} = (2\tilde{\mu})^{1/2} \sup_{\tau \in Z_h(K)} \frac{\langle \lambda, \tau v \rangle_{\partial K}}{\|\tau\|_{0,K}} \lesssim \sup_{\tau \in Z_h(K)} \frac{\langle \lambda, \tau v \rangle_{\partial K}}{\|\tau\|_{\mathcal{A},K}} = \|\lambda\|_{S,K}.$$

Moreover, we have $(\mathcal{A}\sigma_\lambda, \mathbf{I})_K = \langle \lambda, \mathbf{I} v \rangle_{\partial K}$ from (25a). By the Cauchy–Schwarz inequality, we have

$$\begin{aligned} \tilde{\lambda}^{1/2} |\lambda|_{*,K} &= \tilde{\lambda}^{1/2} |K|^{-1/2} |\langle \lambda, \mathbf{I} v \rangle_{\partial K}| = \tilde{\lambda}^{1/2} |K|^{-1/2} |(\mathcal{A}\sigma_\lambda, \mathbf{I})_K| \\ &\leq \tilde{\lambda}^{1/2} |K|^{-1/2} \|\lambda\|_{S,K} (\mathcal{A}\mathbf{I}, \mathbf{I})_K^{1/2} \leq \|\lambda\|_{S,K}. \end{aligned}$$

This completes the proof. \square

Fig. 1 Nearly singular vertex

Next, we estimate the condition number of S . The L^2 norm for $M_{h,k+1}$ is denoted by

$$\|\lambda\|_0^2 := \sum_{F \in \mathcal{F}_h^i} \|\lambda\|_{0,F}^2 := \sum_{F \in \mathcal{F}_h^i} \langle \lambda, \lambda \rangle_F.$$

Lemma 5 *It holds that*

$$\|\lambda\|_S^2 \lesssim (2\tilde{\mu} + \tilde{\lambda})h^{-1}\|\lambda\|_0^2 \quad \forall \lambda \in M_{h,k+1}. \quad (35)$$

Proof The upper bound of S follows from the equivalent norm (33), Cauchy–Schwarz inequality and standard scaling argument. \square

The lower bound of S depends on the singularity of the grids. In light of [49], we define a quantity to measure the vertex singularity. The rest estimates are focused on the case of spatial dimension $n = 2$. For a vertex $a \in \mathcal{N}_h$, let θ_i , $1 \leq i \leq m$ be the angles of the triangle K_i meeting at a (triangles are numbered consecutively). If a is an internal vertex, we define

$$\kappa(a) := \max\{|\theta_i + \theta_j - \pi| \mid 1 \leq i, j \leq m \text{ and } i - j = 1 \pmod{m}\};$$

If a is a boundary vertex, $\kappa(a)$ is defined in the same way without the modulo operation. We call a is a singular vertex if $\kappa(a) = 0$. (We can also give an algebraic definition for the singular vertex, which works for arbitrary spatial dimension. See Appendix A for details.)

We further set

$$\kappa = \min_{a \in \mathcal{N}_h} \kappa(a).$$

In the following, we assume that $\kappa \geq \kappa_0 > 0$, where κ_0 is a positive constant independent of h . That is, there is no singular or nearly singular vertex on T_h (Fig. 1).

Lemma 6 For the 2D case, if there is no interior singular vertex in \mathcal{T}_h , we have $R(\mathcal{C})^\perp = \emptyset$ and $R(\mathcal{C}) = \{\varphi_1, \dots, \varphi_{N_1}\}$ can be chosen such that the mass matrix $\mathbf{M} = (\langle \varphi_i, \varphi_j \rangle_{\mathcal{F}_h^i})$ is well-conditioned, that is,

$$\sum_{i=1}^{N_1} c_i^2 \|\varphi_i\|_0^2 \asymp \left\| \sum_{i=1}^{N_1} c_i \varphi_i \right\|_0^2 \quad \forall (c_1, c_2, \dots, c_{N_1}) \in \mathbb{R}^{N_1}. \quad (36)$$

Proof The detailed proof is given in Appendix B. \square

Lemma 7 Assume that $\kappa \geq \kappa_0 > 0$. For any local basis function φ_i of $R(\mathcal{C})$ (see Lemma 6), there exists a locally supported $\boldsymbol{\tau}_i \in \Sigma_{h,k+1}^{-1}$ such that

$$[\boldsymbol{\tau}_i]|_F = \varphi_i|_F \quad \forall F \in \mathcal{F}_h, \quad \text{and} \quad \|\boldsymbol{\tau}_i\|_0^2 \lesssim \frac{h}{\sin^2(\kappa_0)} \|\varphi_i\|_0^2.$$

Proof The detailed proof is given in Appendix C. \square

Lemma 8 Assume that $\kappa \geq \kappa_0 > 0$. For any $\lambda \in M_{h,k+1}$, there exists $\boldsymbol{\tau} \in \Sigma_{h,k+1}^{-1}$ such that

$$[\boldsymbol{\tau}]|_F = \lambda|_F \quad \forall F \in \mathcal{F}_h, \quad \text{and} \quad \|\boldsymbol{\tau}\|_0^2 \lesssim \frac{h}{\sin^2(\kappa_0)} \|\lambda\|_0^2. \quad (37)$$

Proof Since $\kappa \geq \kappa_0 > 0$, by Lemma 6, we have $M_{h,k+1} = R(\mathcal{C})$ and there exists a local basis that satisfies (36). Therefore, any $\lambda \in M_{h,k+1}$ can be uniquely expressed as

$$\lambda = \sum_{i=1}^{N_1} c_i \varphi_i \quad \text{and} \quad \sum_{i=1}^{N_1} \|c_i \varphi_i\|_0^2 \asymp \|\lambda\|_0^2.$$

By virtue of Lemma 7, there exists a locally supported $\boldsymbol{\tau}_i \in \Sigma_{h,k+1}^{-1}$ for each basis function φ_i of $R(\mathcal{C})$, such that

$$[\boldsymbol{\tau}_i]|_F = \varphi_i|_F \quad \forall F \in \mathcal{F}_h, \quad \text{and} \quad \|\boldsymbol{\tau}_i\|_0^2 \lesssim h \sin^{-2}(\kappa_0) \|\varphi_i\|_0^2.$$

Therefore, $\boldsymbol{\tau} = \sum_{i=1}^{N_1} c_i \boldsymbol{\tau}_i$ satisfies $[\boldsymbol{\tau}]|_F = \lambda$ and

$$\|\boldsymbol{\tau}\|_0^2 \lesssim \sum_{i=1}^{N_1} c_i^2 \|\boldsymbol{\tau}_i\|_0^2 \lesssim h \sin^{-2}(\kappa_0) \sum_{i=1}^{N_1} c_i^2 \|\varphi_i\|_0^2 \asymp h \sin^{-2}(\kappa_0) \|\lambda\|_0^2.$$

This completes the proof. \square

Lemma 9 Assume that $\kappa \geq \kappa_0 > 0$. It holds that

$$2\tilde{\mu}h \sin^2(\kappa_0) \|\lambda\|_0^2 \lesssim \|\lambda\|_S^2 \quad \forall \lambda \in M_{h,k+1}. \quad (38)$$

Proof By virtue of Lemma 8, for any $\lambda \in M_{h,k+1}$, there exists $\boldsymbol{\tau}_1 \in \Sigma_{h,k+1}^{-1}$ such that

$$\mathcal{C}\boldsymbol{\tau}_1 = \lambda \quad \text{and} \quad \|\boldsymbol{\tau}_1\|_0 \lesssim h^{1/2} \sin^{-1}(\kappa_0) \|\lambda\|_0.$$

Applying the discrete inf-sup condition, there exists $\boldsymbol{\tau}_2 \in \Sigma_{h,k+1}$ such that

$$\operatorname{div} \boldsymbol{\tau}_2 = -\operatorname{div}_h \boldsymbol{\tau}_1 \quad \text{and} \quad \|\boldsymbol{\tau}_2\|_{H(\operatorname{div})} \lesssim \|\operatorname{div}_h \boldsymbol{\tau}_1\|_0 \lesssim h^{-1} \|\boldsymbol{\tau}_1\|_0 \lesssim h^{-1/2} \sin^{-1}(\kappa_0) \|\lambda\|_0.$$

Let $\boldsymbol{\tau} = \boldsymbol{\tau}_1 + \boldsymbol{\tau}_2$. Thus, $\operatorname{div}_h \boldsymbol{\tau} = 0$ and $\mathcal{C}\boldsymbol{\tau} = \lambda$. By summation of (25a) over all elements and choosing above $\boldsymbol{\tau}$ as a testing function, we have

$$\|\lambda\|_0^2 = (\mathcal{A}\sigma_\lambda, \boldsymbol{\tau}) \leq (\mathcal{A}\sigma_\lambda, \sigma_\lambda)^{1/2} (2\tilde{\mu})^{-1/2} \|\boldsymbol{\tau}\|_0 \lesssim (2\tilde{\mu}h)^{-1/2} \sin^{-1}(\kappa_0) \|\lambda\|_S \|\lambda\|_0,$$

which implies (38). \square

Lemmas 5 and 9 imply the following condition number estimate:

$$\operatorname{cond}(S) \lesssim \frac{2\tilde{\mu} + \tilde{\lambda}}{2\tilde{\mu}} h^{-2} \sin^{-2}(\kappa_0). \quad (39)$$

For the nearly incompressible material, $\tilde{\lambda}$ would be sufficient large, which makes the multiplier system (28) nearly singular.

4 Multilevel solvers for the hybridized mixed methods

In this section, we shall describe several multilevel solvers for the hybridized mixed methods for the 2D case. We further assume that $\kappa \geq \kappa_0 > 0$, which is guaranteed when the grid has no singular or nearly singular vertex.

4.1 Two-level and multilevel solvers

First, we present the two-level solvers. We consider an overlapping decomposition $\{\Omega_i\}_{i=1}^J$, where Ω_i are open subdomains of Ω . Let \mathcal{T}_H be a coarse grid for Ω , and \mathcal{T}_h be a subdivision of \mathcal{T}_H such that \mathcal{T}_h is aligned with each $\partial\Omega_i$. We assume that there exist nonnegative C^∞ functions $\theta_1, \theta_2, \dots, \theta_J$ in \mathbb{R}^2 such that

$$\theta_i = 0 \quad \text{on } \Omega \setminus \Omega_i, \quad (40a)$$

$$\sum_{i=1}^J \theta_i = 1 \quad \text{on } \bar{\Omega}, \quad (40b)$$

$$\|\nabla \theta_i\|_\infty \lesssim \delta^{-1}. \quad (40c)$$

Here, $\delta > 0$ is a parameter that measures the overlap among the subdomains. We also assume that there exists an integer N_c independent of h, δ , and J such that any point

in Ω belongs to at most N_c subdomains. The local space associated with subdomain Ω_i is denoted by

$$M_i := \{\lambda \in M_{h,k+1} \mid \lambda|_F = 0, \text{ for any face } F \in \Omega \setminus \Omega_i\}. \quad (41)$$

We can then define $S_i : M_i \mapsto M'_i$ and bilinear form on M_i by

$$\langle S_i \lambda_i, \mu_i \rangle := s_i(\lambda_i, \mu_i) := s(\iota_i \lambda_i, \iota_i \mu_i),$$

where $\iota_i : M_i \hookrightarrow M_{h,k+1}$ denotes the inclusion operator.

In light of the multigrid method on the primal elasticity problem by Schöberl [47], we choose the continuous and piecewise quadratic finite element space as the coarse space

$$W_H := \{w \in H_0^1(\Omega; \mathbb{R}^2) \mid w|_K \in \mathcal{P}_2(K; \mathbb{R}^2) \quad \forall K \in \mathcal{T}_H\}.$$

Suppose the coarse space W_H is connected to $M_{h,k+1}$ by an injective intergrid operator $I_H^h : W_H \mapsto M_{h,k+1}$ (The construction of I_H^h will be given in Sect. 4.2). We will impose the primal elastic norm $\|\cdot\|_{A_H}$ on W_H , where $A_H : W_H \mapsto W'_H$ and the bilinear form $a_H(\cdot, \cdot)$ are defined as

$$\begin{aligned} \langle A_H w_H, v_H \rangle &:= a_H(w_H, v_H) \\ &:= 2\tilde{\mu}(\boldsymbol{\varepsilon}(w_H), \boldsymbol{\varepsilon}(v_H)) + \tilde{\lambda}(P_0^H \operatorname{div} w_H, P_0^H \operatorname{div} v_H) \quad \forall w_H, v_H \in W_H, \\ \|w_H\|_{A_H}^2 &:= a_H(w_H, w_H) \quad \forall w_H \in W_H. \end{aligned} \quad (42)$$

Here, P_0^H is the L^2 projection on the piecewise constant space on \mathcal{T}_H . Then, the two-level additive Schwarz preconditioner can be constructed as

$$B_{\text{ad}} = I_H^h A_H^{-1} (I_H^h)' + \sum_{i=1}^J \iota_i S_i^{-1} \iota_i'. \quad (43)$$

Our main contribution is the following estimate.

Theorem 7 *The condition number of $B_{\text{ad}} S$ satisfies*

$$\operatorname{cond}(B_{\text{ad}} S) \leq C(1 + N_c) \frac{H^2}{\delta^2},$$

where C is independent to both the mesh size h and the Lamé constants.

According to [52,54], the estimate of the condition number of the additive Schwarz method is based on the stability of the intergrid transfer operator I_H^h (Lemma 10) and the stable decomposition (Theorem 9), which will be proved in the rest of this section.

Now, we are ready to introduce the multilevel preconditioner as follows:

$$\tilde{B}_{\text{ad}} = I_H^h B_H (I_H^h)' + \sum_{i=1}^J \iota_i S_i^{-1} \iota_i'. \quad (44)$$

Here, $B_H : W'_H \mapsto W_H$ is the multilevel preconditioner for A_H , see [47,48]. Then we have the following theorem.

Theorem 8 *If*

$$\langle B_H^{-1} w_H, w_H \rangle \approx \langle A_H w_H, w_H \rangle \quad \forall w_H \in W_H,$$

then the condition number of $\tilde{B}_{\text{ad}} S$ satisfies

$$\text{cond}(\tilde{B}_{\text{ad}} S) \leq C(1 + N_c) \frac{H^2}{\delta^2},$$

where C is independent to the mesh size h and the Lamé constants.

Proof It follows directly from Theorem 7 and norm equivalence between $\|\cdot\|_{A_H}$ and $\|\cdot\|_{B_H^{-1}}$. \square

- Remark 3**
1. When $H \lesssim \delta$, the preconditioners (43) and (44) are both uniform with respect to h and the Lamé constants.
 2. It can be proved that the corresponding multiplicative preconditioners are also uniform as well as the additive version, provided that the local problems associated with the subdomains are solved exactly (cf. [3,21,37]).
 3. Some robust multilevel methods to solve the linear elasticity problem can be found in [16,20,25,30,39]. By constructing stable intergrid transfer operators similar to I_H^h , it is feasible to construct corresponding multilevel solvers to the hybridized mixed method.

4.2 Intergrid transfer operator I_H^h

The construction of intergrid transfer operator I_H^h is divided into two steps: (i) the intergrid transfer operator from coarse grid to fine grid proposed by Schöberl [47], and (ii) the L^2 projection operator to Lagrange multiplier space. More precisely, we first define the \mathcal{P}_2 Lagrange finite element space W_h on \mathcal{T}_h

$$W_h := \{w \in H_0^1(\Omega; \mathbb{R}^2) \mid w|_K \in \mathcal{P}_2(K; \mathbb{R}^2) \quad \forall K \in \mathcal{T}_h\},$$

with the primal elastic norm $\|\cdot\|_{A_h}$, bilinear form $a_h(\cdot, \cdot)$, and $A_h : W_h \mapsto W'_h$ similar to (42). In [47], the harmonic extension $\tilde{I}_H^h : W_H \mapsto W_h$ was defined as follows: For $w_H \in W_H$, the value of $\tilde{I}_H^h w_H$ on each edge of coarse element $K_H \in \mathcal{T}_H$ does not

change, and the value in the interior of K_H is defined by discrete harmonic extension, that is,

$$\begin{aligned} \tilde{I}_H^h w_H|_{\partial K_H} &= w_H|_{\partial K_H}, \\ a_h(\tilde{I}_H^h w_H, v_h) &= 0 \quad \forall v_h \in W_{h,0}(K_H), \end{aligned} \quad (45)$$

where $W_{h,0}(K_H) := \{w \in H_0^1(K_H; \mathbb{R}^2) \mid w|_{K'} \in \mathcal{P}_2(K'; \mathbb{R}^2) \quad \forall K' \in K_H\}$. \tilde{I}_H^h has the following stability property (cf. [47]),

$$\|\tilde{I}_H^h w_H\|_{A_h} \lesssim \|w_H\|_{A_H} \quad \forall w_H \in W_H. \quad (46)$$

The intergrid transfer operator I_H^h appearing in (43) is defined as the product of two operators,

$$I_H^h := Q_h \tilde{I}_H^h : W_H \mapsto M_{h,k+1}, \quad (47)$$

where $Q_h : W_h \mapsto M_{h,k+1}$ is the L^2 projection on edges (i.e., $\langle Q_h w_h, \mu \rangle_{\mathcal{F}_h} := \langle w_h, \mu \rangle_{\mathcal{F}_h}, \forall \mu \in M_{h,k+1}$). Then, we have the following lemma:

Lemma 10 *The intergrid transfer operator $I_H^h : W_H \mapsto M_{h,k+1}$ has the following stability property:*

$$\|I_H^h w_H\|_S \lesssim \|w_H\|_{A_H} \quad \forall w_H \in W_H. \quad (48)$$

Proof Note that Q_h is the L^2 projection on $M_{h,k+1}$. Then, for any $w_h \in W_h$,

$$\begin{aligned} |Q_h w_h|_{*,K} &= |K|^{-1/2} \left| \int_{\partial K} Q_h w_h \cdot v \, ds \right| = |K|^{-1/2} \left| \int_{\partial K} w_h \cdot v \, ds \right| \\ &= |K|^{-1/2} \left| \int_K \operatorname{div} w_h \, dx \right| = \|P_0^h \operatorname{div} w_h\|_{0,K}, \end{aligned}$$

and

$$\begin{aligned} |Q_h w_h|_{h,K} &= \sup_{\boldsymbol{\tau} \in Z_h(K)} \frac{\langle Q_h w_h, \boldsymbol{\tau} v \rangle_{\partial K}}{\|\boldsymbol{\tau}\|_{0,K}} = \sup_{\boldsymbol{\tau} \in Z_h(K)} \frac{\langle w_h, \boldsymbol{\tau} v \rangle_{\partial K}}{\|\boldsymbol{\tau}\|_{0,K}} \\ &= \sup_{\boldsymbol{\tau} \in Z_h(K)} \frac{(\varepsilon(w_h), \boldsymbol{\tau})_K}{\|\boldsymbol{\tau}\|_{0,K}} \leq \|\varepsilon(w_h)\|_{0,K}, \end{aligned}$$

which implies that $\|Q_h w_h\|_S \lesssim \|w_h\|_{A_h}$ due to Theorem 6. The stability property (48) then follows from (46) and the stability property of Q_h . \square

4.3 Stable decomposition

In this section, we shall present the stable decomposition. A key tool to prove the stable decomposition is the interpolation $\Pi_h : M_{h,k+1} \mapsto W_h$, which is used to capture the low-frequency of the multiplier $\lambda \in M_{h,k+1}$.

We first define a parameter-independent problem: Find $(\bar{\sigma}_\lambda, \bar{u}_\lambda) \in \Sigma_{h,k+1}^{-1} \times V_{h,k}$ such that for any element $K \in \mathcal{T}_h$,

$$(\bar{\sigma}_\lambda, \tau_h)_K + (\bar{u}_\lambda, \operatorname{div} \tau_h)_K = \langle \lambda, \tau_h v \rangle_{\partial K} \quad \forall \tau_h \in \mathcal{P}_{k+1}(K; \mathbb{S}), \quad (49a)$$

$$(\operatorname{div} \bar{\sigma}_\lambda, v_h)_K = 0 \quad \forall v_h \in \mathcal{P}_k(K; \mathbb{R}^2). \quad (49b)$$

We then introduce the following rigid motion space on each element K ,

$$\operatorname{RM}(K) := \{v \in H^1(K, \mathbb{R}^2) \mid (\nabla v + (\nabla v)^T)/2 = 0\}. \quad (50)$$

We also introduce a projection $P_{K,\operatorname{RM}} : M_{h,k+1}(\partial K) \mapsto \operatorname{RM}(K)$ by

$$(P_{K,\operatorname{RM}}\lambda, r)_K = (\bar{u}_\lambda, r)_K \quad \forall r \in \operatorname{RM}(K). \quad (51)$$

Then, the construction of the interpolation Π_h is divided into two steps. First, a Clément type interpolation $\Pi_{1,h} : M_{h,k+1} \mapsto (\mathcal{P}_{1,h})^2 \cap H^1(\Omega; \mathbb{R}^2)$ is defined as, for any $a \in \mathcal{N}_h$,

$$(\Pi_{1,h}\lambda)(a) := \begin{cases} \frac{\sum_{K \in \omega_a} (P_{K,\operatorname{RM}}\lambda)(a)}{\sum_{K \in \omega_a} 1} & a \notin \partial\Omega, \\ 0 & a \in \partial\Omega, \end{cases}$$

where $\mathcal{P}_{1,h}$ is the piecewise linear Lagrange element and ω_a is the set of elements containing the vertex a . Next, we define the correction operator $\Pi_{2,h} : M_{h,k+1} \cup H_1(\Omega, \mathbb{R}^2) \mapsto W_h$:

$$(\Pi_{2,h}\lambda)(a) := 0 \quad \forall a \in \mathcal{N}_h, \quad \text{and} \quad \int_F \Pi_{2,h}\lambda \, ds := \int_F \lambda \, ds \quad \forall F \in \mathcal{F}_h.$$

Then, the interpolation Π_h is composed by these two operators,

$$\Pi_h\lambda := \Pi_{1,h}\lambda + \Pi_{2,h}(\lambda - \Pi_{1,h}\lambda) \quad \forall \lambda \in M_{h,k+1}. \quad (52)$$

Note that the interpolation Π_h is only used for analysis and will not occur in the computation. To prove the stability and approximation property of Π_h , we present some lemmas on $P_{K,\operatorname{RM}}$.

Lemma 11 *It holds that*

$$h_K^{-1} \|\bar{u}_\lambda - P_{K,\operatorname{RM}}\lambda\|_{0,K} \lesssim |\lambda|_{h,K}. \quad (53)$$

Proof By definition, we have $(\bar{u}_\lambda - P_{K,\text{RM}}\lambda) \in \text{RM}(K)^\perp$. According to the Theorem 2.2 in [31], we can find $\tilde{\boldsymbol{\tau}}_h \in \Sigma_{k+1,b}(K)$ such that

$$\operatorname{div}\tilde{\boldsymbol{\tau}}_h = \bar{u}_\lambda - P_{K,\text{RM}}\lambda \quad \text{and} \quad h_K^{-1}\|\tilde{\boldsymbol{\tau}}_h\|_{0,K} \lesssim \|\operatorname{div}\tilde{\boldsymbol{\tau}}_h\|_0 = \|\bar{u}_\lambda - P_{K,\text{RM}}\lambda\|_{0,K}.$$

Since $\tilde{\boldsymbol{\tau}}_h v|_{\partial K} = 0$, (49a) implies that

$$(\bar{\boldsymbol{\sigma}}_\lambda, \tilde{\boldsymbol{\tau}}_h)_K + (\bar{u}_\lambda - P_{K,\text{RM}}\lambda, \operatorname{div}\tilde{\boldsymbol{\tau}}_h)_K = 0.$$

Thus,

$$\begin{aligned} \|\bar{u}_\lambda - P_{K,\text{RM}}\lambda\|_{0,K}^2 &= (\bar{u}_\lambda - P_{K,\text{RM}}\lambda, \operatorname{div}\tilde{\boldsymbol{\tau}}_h)_K = -(\bar{\boldsymbol{\sigma}}_\lambda, \tilde{\boldsymbol{\tau}}_h) \leq \|\bar{\boldsymbol{\sigma}}_\lambda\|_{0,K} \|\tilde{\boldsymbol{\tau}}_h\|_{0,K} \\ &\lesssim h_K \|\bar{u}_\lambda - P_{K,\text{RM}}\lambda\|_{0,K} \|\bar{\boldsymbol{\sigma}}_\lambda\|_{0,K}. \end{aligned}$$

Note that $\bar{\boldsymbol{\sigma}}_\lambda \in Z_h(K)$ by (49b). By definition of $|\cdot|_{h,K}$ in (31), we have

$$|\lambda|_{h,K} = \sup_{\boldsymbol{\tau}_h \in Z_h(K)} \frac{\langle \lambda, \boldsymbol{\tau}_h v \rangle_{\partial K}}{\|\boldsymbol{\tau}_h\|_{0,K}} = \sup_{\boldsymbol{\tau}_h \in Z_h(K)} \frac{(\bar{\boldsymbol{\sigma}}_\lambda, \boldsymbol{\tau}_h)_K}{\|\boldsymbol{\tau}_h\|_{0,K}} = \|\bar{\boldsymbol{\sigma}}_\lambda\|_{0,K}.$$

Then, (53) follows from the above two equations. \square

Lemma 12 Assume that $\kappa \geq \kappa_0 > 0$. It holds that

$$h_K^{-1}\|\lambda - P_{K,\text{RM}}\lambda\|_{0,\partial K}^2 \lesssim \sum_{K' \in \omega_K} |\lambda|_{h,K'}^2. \quad (54)$$

Proof By virtue of Lemma 11, the triangle inequality, and the trace inequality, we only need to prove

$$h_K^{-1}\|\lambda - \bar{u}_\lambda\|_{0,\partial K}^2 \lesssim \sum_{K' \in \omega_K} |\lambda|_{h,K'}^2. \quad (55)$$

Consider the element patch ω_K . Let $\mathcal{F}_h(\omega_K) := \mathcal{F}_h \cap \bar{\omega}_K$ and $\Sigma_{h,k+1}^{-1}(\omega_K) := \{\boldsymbol{\tau}_h \in L^2(\omega_K; \mathbb{S}) \mid \boldsymbol{\tau}_h|_K' \in \mathcal{P}_{k+1}(K'; \mathbb{S}) \quad \forall K' \in \omega_K\}$. By summation of (49a) over elements $K' \in \omega_K$, we have

$$(\bar{\boldsymbol{\sigma}}_\lambda, \boldsymbol{\tau}_h)_{\omega_K} + (\bar{u}_\lambda, \operatorname{div}_h \boldsymbol{\tau}_h)_{\omega_K} = \sum_{K' \in \omega_K} \langle \lambda, \boldsymbol{\tau}_h v \rangle_{\partial K'} \quad \forall \boldsymbol{\tau}_h \in \Sigma_{h,k+1}^{-1}(\omega_K). \quad (56)$$

Note that $\bar{u}_\lambda|_K \in \mathcal{P}_k(K; \mathbb{R}^2)$, we denote by \bar{u}_K the natural continuous extension of $\bar{u}_\lambda|_K$ on ω_K (i.e., \bar{u}_K and $\bar{u}_\lambda|_K$ have the same polynomial form). Then, we can recast (56) as

$$(\bar{\boldsymbol{\sigma}}_\lambda, \boldsymbol{\tau}_h)_{\omega_K} + (\bar{u}_\lambda - \bar{u}_K, \operatorname{div}_h \boldsymbol{\tau}_h)_{\omega_K} - (\varepsilon(\bar{u}_K), \boldsymbol{\tau}_h)_{\omega_K} = \sum_{F \in \mathcal{F}_h(\omega_K)} \langle \lambda - \bar{u}_K, [\boldsymbol{\tau}_h] \rangle_F. \quad (57)$$

Since $\kappa \geq \kappa_0 > 0$, by Lemma 8, there exists $\boldsymbol{\tau}_1 \in \Sigma_{h,k+1}^{-1}(\omega_K)$ such that

$$[\boldsymbol{\tau}_1]_F = \begin{cases} (\lambda - u_K)|_F & F \in \partial K, \\ 0 & \text{otherwise,} \end{cases} \quad \text{and} \quad \|\boldsymbol{\tau}_1\|_{0,\omega_K}^2 \lesssim h_K \sin^{-2}(\kappa_0) \|\lambda - u_K\|_{0,\partial K}^2. \quad (58)$$

Apply Lemmas 1 or 2 on ω_K , we immediately know that there exists $\boldsymbol{\tau}_2 \in \Sigma_{h,k+1}(\omega_K) := \{\boldsymbol{\tau} \in H(\text{div}, \omega_K; \mathbb{S}) \mid \boldsymbol{\tau}|_{K'} \in \mathcal{P}_{k+1}(K'; \mathbb{S}) \quad \forall K' \in \omega_K\}$ such that

$$\text{div} \boldsymbol{\tau}_2 = -\text{div}_h \boldsymbol{\tau}_1 \quad \text{and} \quad h_K^{-1} \|\boldsymbol{\tau}_2\|_{0,\omega_K} + \|\text{div} \boldsymbol{\tau}_2\|_{0,\omega_K} \lesssim \|\text{div} \boldsymbol{\tau}_1\|_{0,\omega_K} \lesssim h_K^{-1} \|\boldsymbol{\tau}_1\|_{0,\omega_K}. \quad (59)$$

Next, there is a unique decomposition that $\bar{u}_K|_K = \theta_1 + \theta_2 \in \text{RM}(K) \oplus \text{RM}(K)^\perp$. Due to Theorem 2.2 in [31], we can find $\tilde{\boldsymbol{\tau}}_3 \in \Sigma_{k+1,b}(K)$ such that

$$\text{div} \tilde{\boldsymbol{\tau}}_3 = \theta_2 \quad \text{and} \quad h_K^{-1} \|\tilde{\boldsymbol{\tau}}_3\|_{0,K} \lesssim \|\theta_2\|_{0,K}.$$

Let $\text{supp}(\boldsymbol{\tau}_3) \subset K$ and

$$\boldsymbol{\tau}_3|_K = \begin{cases} \frac{(\boldsymbol{\tau}_1 + \boldsymbol{\tau}_2, \varepsilon(\bar{u}_K))_{\omega_K}}{\|\theta_2\|_{0,K}^2} \tilde{\boldsymbol{\tau}}_3 & \theta_2 \neq 0, \\ \mathbf{0} & \theta_2 = 0. \end{cases}$$

A straightforward calculation shows that $\boldsymbol{\tau}_3$ satisfies

$$-(\boldsymbol{\tau}_3, \varepsilon(\bar{u}_K))_K = (\text{div} \boldsymbol{\tau}_3, \theta_2)_K = (\boldsymbol{\tau}_1 + \boldsymbol{\tau}_2, \varepsilon(\bar{u}_K))_{\omega_K}, \quad (60)$$

and

$$\begin{aligned} \|\boldsymbol{\tau}_3\|_{0,K} &\leq \|\boldsymbol{\tau}_1 + \boldsymbol{\tau}_2\|_{0,\omega_K} \frac{\|\varepsilon(\bar{u}_K)\|_{0,\omega_K} \|\tilde{\boldsymbol{\tau}}_3\|_{0,K}}{\|\theta_2\|_{0,K}^2} \\ &\lesssim \|\boldsymbol{\tau}_1 + \boldsymbol{\tau}_2\|_{0,\omega_K} \frac{h_K \|\varepsilon(\bar{u}_K)\|_{0,K}}{\|\theta_2\|_{0,K}} \lesssim \|\boldsymbol{\tau}_1 + \boldsymbol{\tau}_2\|_{0,\omega_K}. \end{aligned} \quad (61)$$

Thus, take $\boldsymbol{\tau} = \boldsymbol{\tau}_1 + \boldsymbol{\tau}_2 + \boldsymbol{\tau}_3$ in (57), we have

$$[\boldsymbol{\tau}]_F = \begin{cases} (\lambda - u_K)|_F & F \in \partial K, \\ 0 & \text{otherwise,} \end{cases} \quad (\bar{u}_\lambda - \bar{u}_K, \text{div} \boldsymbol{\tau})_{\omega_K} = 0 \quad \text{and} \quad (\varepsilon(\bar{u}_K), \boldsymbol{\tau})_{\omega_K} = 0.$$

In addition, (58), (59), and (61) imply that

$$\|\boldsymbol{\tau}\|_{0,\omega_K} \lesssim \|\boldsymbol{\tau}_1\|_{0,\omega_K} \lesssim h_K^{1/2} \sin^{-1}(\kappa_0) \|\lambda - \bar{u}_K\|_{0,\partial K}.$$

Hence, we have

$$\begin{aligned} \|\lambda - \bar{u}_K\|_{0,\partial K}^2 &= (\bar{\sigma}_\lambda, \tau)_{\omega_K} \lesssim \|\bar{\sigma}_\lambda\|_{0,\omega_K} \|\tau\|_{0,\omega_K} \\ &\lesssim \left(\sum_{K' \in \omega_K} |\lambda|_{h,K'}^2 \right)^{1/2} h_K^{1/2} \sin^{-1}(\kappa_0) \|\lambda - u_K\|_{0,\partial K}, \end{aligned}$$

which gives rise to (55). \square

Now, we are in the place to prove the stability and approximation property of Π_h .

Lemma 13 *For any $\lambda \in M_{h,k+1}$, it holds that*

$$\int_F \Pi_h \lambda \, ds = \int_F \lambda \, ds \quad \forall F \in \mathcal{F}_h, \quad (62)$$

$$\|\Pi_h \lambda\|_{A_h} \lesssim \|\lambda\|_S, \quad (63)$$

$$\|\lambda - Q_h \Pi_h \lambda\|_0^2 \lesssim h \|\lambda\|_S^2. \quad (64)$$

Proof By the definition of Π_h in (52), we have

$$\int_F \lambda - \Pi_h \lambda \, ds = \int_F (I - \Pi_{2,h})(I - \Pi_{1,h})\lambda \, ds = 0,$$

which gives rise to (62).

Since $\|\Pi_h \lambda\|_{A_h}^2 = 2\tilde{\mu} \|\varepsilon(\Pi_h \lambda)\|_0^2 + \tilde{\lambda} \|P_0^h \operatorname{div}(\Pi_h \lambda)\|_0^2$, we prove the stability (63) of Π_h part by part. By (62), we have

$$\begin{aligned} \|P_0^h \operatorname{div} \Pi_h \lambda\|_{0,K} &= |K|^{-1/2} \left| \int_K \operatorname{div}(\Pi_h \lambda) \, dx \right| = |K|^{-1/2} \left| \int_{\partial K} (\Pi_h \lambda) \cdot v \, ds \right| \\ &= |K|^{-1/2} \left| \int_{\partial K} \lambda \cdot v \, ds \right| = |\lambda|_{*,K}. \end{aligned} \quad (65)$$

Next, we estimate $\|\varepsilon(\Pi_h \lambda)\|_{0,K}$. First, we show the stability of $\Pi_{1,h}$ as

$$\begin{aligned} \|\Pi_{1,h} \lambda - P_{K,\text{RM}} \lambda\|_{0,K}^2 &\lesssim h_K^n \sum_{a \in \mathcal{N}_K} |(\Pi_{1,h} \lambda)(a) - (P_{K,\text{RM}} \lambda)(a)|^2 \\ &\lesssim h_K^n \sum_{a \in \mathcal{N}_K} \sum_{\substack{\tilde{K}_1 \cap \tilde{K}_2 = \tilde{F} \\ \tilde{F} \ni a}} |(P_{K_1,\text{RM}} \lambda)(a) - (P_{K_2,\text{RM}} \lambda)(a)|^2 \\ &\lesssim h_K^n \sum_{a \in \mathcal{N}_K} \sum_{\substack{\tilde{K}_1 \cap \tilde{K}_2 = \tilde{F} \\ \tilde{F} \ni a}} |\lambda|_F(a) - (P_{K_1,\text{RM}} \lambda)(a)|^2 + |\lambda|_F(a) - (P_{K_2,\text{RM}} \lambda)(a)|^2 \end{aligned}$$

$$\begin{aligned}
&\lesssim \sum_{a \in \mathcal{N}_K} \sum_{\substack{\tilde{K}_1 \cap \tilde{K}_2 = \tilde{F} \\ \tilde{F} \ni a}} h_{K_1} \|\lambda - P_{K_1, \text{RM}} \lambda\|_{0, \partial K_1}^2 + h_{K_2} \|\lambda - P_{K_2, \text{RM}} \lambda\|_{0, \partial K_2}^2 \\
&\lesssim \sum_{K' \in \omega_K} h_{K'} \|\lambda - P_{K', \text{RM}} \lambda\|_{0, \partial K'}^2. \tag{66}
\end{aligned}$$

Then, by the triangle inequality and inverse inequality, we have

$$\begin{aligned}
\|\Pi_h \lambda - P_{K, \text{RM}} \lambda\|_{0, K}^2 &\lesssim \|\Pi_h \lambda - \Pi_{1, h} \lambda\|_{0, K}^2 + \|\Pi_{1, h} \lambda - P_{K, \text{RM}} \lambda\|_{0, K}^2 \\
&= \|\Pi_{2, h}(I - \Pi_{1, h})\lambda\|_{0, K}^2 + \|\Pi_{1, h}\lambda - P_{K, \text{RM}} \lambda\|_{0, K}^2 \\
&\lesssim h_K \|(I - \Pi_{1, h})\lambda\|_{0, \partial K}^2 + \|\Pi_{1, h}\lambda - P_{K, \text{RM}} \lambda\|_{0, K}^2 \\
&\lesssim \sum_{K' \in \omega_K} h_{K'} \|\lambda - P_{K', \text{RM}} \lambda\|_{0, \partial K'}^2. \quad (\text{by (66)}) \tag{67}
\end{aligned}$$

Hence, by the inverse inequality, we have

$$\begin{aligned}
\|\varepsilon(\Pi_h \lambda)\|_{0, K}^2 &= \|\varepsilon(\Pi_h \lambda - P_{K, \text{RM}} \lambda)\|_{0, K}^2 \\
&\lesssim h_K^{-2} \|\Pi_h \lambda - P_{K, \text{RM}} \lambda\|_{0, K}^2 \\
&\lesssim \sum_{K' \in \omega_K} h_{K'}^{-1} \|\lambda - P_{K', \text{RM}} \lambda\|_{0, \partial K'}^2. \quad (\text{by (67)}) \tag{68}
\end{aligned}$$

By virtue of (54), we sum (65) and (68) over all elements to obtain

$$\|\Pi_h \lambda\|_{A_h} \lesssim \|\lambda\|_S.$$

Next, the approximation property (64) can be obtained by summing the following inequalities over all elements:

$$\begin{aligned}
\|\lambda - Q_h \Pi_h \lambda\|_{0, \partial K}^2 &\lesssim \|(I - Q_h)\Pi_h \lambda\|_{0, \partial K}^2 + \|\lambda - P_{K, \text{RM}} \lambda\|_{0, \partial K}^2 + \|P_{K, \text{RM}} \lambda - \Pi_h \lambda\|_{0, \partial K}^2 \\
&\lesssim h_K^4 |\Pi_h \lambda|_{2, \partial K}^2 + \sum_{K' \in \omega_K} \|\lambda - P_{K', \text{RM}} \lambda\|_{0, \partial K'}^2 \quad (\text{by (67)}) \\
&\lesssim h_K \|\varepsilon(\Pi_h \lambda)\|_{0, K}^2 + \sum_{K' \in \omega_K} \|\lambda - P_{K', \text{RM}} \lambda\|_{0, \partial K'}^2. \tag{69}
\end{aligned}$$

This completes the proof. \square

Let $\{W_i\}_{i=1}^J$ be the local spaces of W_h associated with the overlapping domain decomposition $\{\Omega_i\}_{i=1}^J$. According to [48], we have the following lemma.

Lemma 14 *For any $w_h \in W_h$, there exists a decomposition $w_h = \tilde{I}_H^h w_H + \sum_{i=1}^J w_i$, such that $w_H \in W_H$, $w_i \in W_i$, and*

$$\|w_H\|_{A_H}^2 + \sum_{i=1}^J \|w_i\|_{A_h}^2 \lesssim \frac{H^2}{\delta^2} \|w_h\|_{A_h}^2. \tag{70}$$

Theorem 9 For any $\lambda \in M_{h,k+1}$, there exists a decomposition $\lambda = I_H^h w_H + \sum_{i=1}^J \lambda_i$ such that $w_H \in W_H$, $\lambda_i \in M_i$, and

$$\|w_H\|_{A_H}^2 + \sum_{i=1}^J \|\lambda_i\|_S^2 \lesssim \frac{H^2}{\delta^2} \|\lambda\|_S^2. \quad (71)$$

Proof We first split λ into two components

$$\lambda = Q_h \underbrace{\Pi_h \lambda}_{w_h} + \underbrace{(\lambda - Q_h \Pi_h \lambda)}_{\lambda_0}.$$

According to the Lemma 13, we know that

$$\lambda_0 \in M_{h,0}^\perp \quad \text{and} \quad \|\lambda_0\|_0^2 \lesssim h \|\lambda\|_S^2.$$

Here, $M_{h,0}^\perp$ is the L^2 orthogonal complement of $M_{h,0}$ in the space $M_{h,k+1}$. Denote the L^2 projection on $M_{h,0}^\perp$ by Q_0^\perp . Let $w_h = I_H^h w_H + \sum_{i=1}^J w_i$ be the decomposition in Lemma 14. We define the λ_i as

$$\lambda_i = Q_h w_i + Q_0^\perp(\theta_i \lambda_0) \quad j = 1, 2, \dots, J.$$

Thus, $\lambda = I_H^h w_H + \sum_{i=1}^J \lambda_i$. By the property of the partition of unity, Theorem 6, Lemmas 10, 13, and 14, we have

$$\begin{aligned} \sum_{i=1}^J \|\lambda_i\|_S^2 &= \sum_{i=1}^J \sum_{K \in \mathcal{T}_h \cap \Omega_i} \|\lambda_i\|_{S,K}^2 \\ &\lesssim \sum_{i=1}^J \|Q_h w_i\|_S^2 + \sum_{i=1}^J \sum_{K \in \mathcal{T}_h \cap \Omega_i} \|Q_0^\perp(\theta_i \lambda_0)\|_{S,K}^2 \\ &\lesssim \sum_{i=1}^J \|Q_h w_i\|_S^2 + \sum_{i=1}^J \sum_{K \in \mathcal{T}_h \cap \Omega_i} h_K^{-1} \|Q_0^\perp(\theta_i \lambda_0)\|_{0,\partial K}^2 \quad (\text{by (33)}) \\ &\lesssim \sum_{i=1}^J \|Q_h w_i\|_S^2 + h^{-1} \|\lambda_0\|_0^2 \\ &\lesssim \frac{H^2}{\delta^2} \|w_h\|_{A_h}^2 + h^{-1} \|\lambda_0\|_0^2 \quad (\text{by Lemma 10 and (70)}) \\ &\lesssim \frac{H^2}{\delta^2} \|\lambda\|_S^2, \quad (\text{by (63) and (64)}) \end{aligned}$$

and

$$\|w_H\|_{A_H} \lesssim \frac{H^2}{\delta^2} \|w_h\|_{A_h} \lesssim \frac{H^2}{\delta^2} \|\lambda\|_S.$$

This completes the proof. \square

Table 2 Errors and observed convergence orders on HCT grids, $k = 0$, 2D

$1/h$	$\ u - u_h\ _0$	Order	$\ \sigma - \sigma_h\ _0$	Order	$\ \operatorname{div}\sigma - \operatorname{div}\sigma_h\ _0$	Order
4	9.5309e-2	–	2.0147e-1	–	2.6589e-0	–
8	4.5289e-2	1.07	4.9971e-2	2.01	1.2995e-0	1.03
16	2.2009e-2	1.04	1.2357e-2	2.01	6.3735e-1	1.02
32	1.0976e-2	1.00	3.1761e-3	1.96	3.1827e-1	1.00
64	5.4797e-3	1.00	8.0961e-4	1.97	1.5892e-1	1.00

5 Numerical examples

In this section, we give several numerical examples to present the optimal convergence order of the hybridized mixed discretization as well as the uniform convergence of the iterative solvers. All the numerical experiments are implemented using the iFEM package [19].

5.1 Convergence order tests

To verify the convergence order for the discretization, we take the domain to be unit square $\Omega = (0, 1)^2$ or unit cube $\Omega = (0, 1)^3$, and choose the data with the exact solutions given by

$$u = \begin{cases} (xy(1-x)(1-y)e^{x-y}, \sin(\pi x) \sin(\pi y))^T & \text{for 2D,} \\ x(1-x)y(1-y)z(1-z)(2^4, 2^5, 2^6)^T & \text{for 3D.} \end{cases} \quad (72)$$

We apply a homogeneous boundary condition that $u = 0$ on $\partial\Omega$. The Lamé constants are set as $\tilde{\mu} = 1/2$ and $\tilde{\lambda} = 1$. The exact stress function σ and the load function f can be analytically derived from the (1) for a given u . In all the numerical tests, we assemble the linear systems of the Lagrange multiplier directly and recover the primal unknowns (the stress and displacement) locally after solving the Lagrange multiplier.

Example 1 (2D tests) Our first numerical example is carried out for the lowest order case ($k = 0$) on the HCT grids, which can be obtained from any triangulation by connecting the vertices of each triangle to the barycenter. After computing (21) for various values of h , we calculate the errors between the exact solution and the discrete solution and report them in Table 2. The table indicates the optimal convergence orders of $\mathcal{O}(h)$ for both stress and displacement in the $H(\operatorname{div})$ and L^2 norm, respectively.

We also apply the hybridized mixed method with $k = 2$ for the high order case, which is the lowest order method that works for any 2D regular grid. We perform the test of high order on uniform grids. Table 3 indicates the optimal convergence for the high order case $k = 2$. We use the MATLAB backslash solver in these two tests since the multiplier systems are SPD.

Table 3 Errors and observed convergence orders on uniform grids, $k = 2$, 2D

$1/h$	$\ u - u_h\ _0$	Order	$\ \sigma - \sigma_h\ _0$	Order	$\ \operatorname{div}\sigma - \operatorname{div}\sigma_h\ _0$	Order
4	2.1758e-3	–	2.0260e-3	–	6.2558e-2	–
8	2.7561e-4	2.98	1.5145e-4	3.89	7.9274e-3	2.98
16	3.4569e-5	2.99	9.7454e-6	3.95	9.9431e-4	2.99
32	4.3248e-6	2.99	6.1737e-7	3.98	1.2439e-4	3.00
64	5.4072e-7	3.00	3.8838e-8	3.99	1.5552e-5	3.00

Table 4 Errors and observed convergence orders on HCT grids, $k = 1$, 3D

$1/h$	$\ u - u_h\ _0$	Order	$\ \sigma - \sigma_h\ _0$	Order	$\ \operatorname{div}\sigma - \operatorname{div}\sigma_h\ _0$	Order
2	6.1603e-2	–	2.2087e-1	–	2.1633e-0	–
4	1.6850e-2	1.87	3.4925e-2	2.66	5.7599e-1	1.91
8	4.3164e-3	1.96	4.7963e-3	2.86	1.4620e-1	1.98

Table 5 Errors and observed convergence orders on uniform grids, $k = 3$, 3D

$1/h$	$\ u - u_h\ _0$	Order	$\ \sigma - \sigma_h\ _0$	Order	$\ \operatorname{div}\sigma - \operatorname{div}\sigma_h\ _0$	Order
2	4.1578e-3	–	6.6227e-3	–	9.2034e-2	–
4	2.8154e-4	3.88	2.3795e-4	4.80	5.7521e-3	4.00
8	1.7958e-5	3.97	8.0101e-6	4.89	3.5951e-4	4.00

Example 2 (3D tests) We carry out two tests for the 3D case: one for the lowest order $k = 1$ on the HCT grids, the other for the higher order $k = 3$ on the uniform grids. We list the errors and observed convergence orders of the computed solutions in Table 4 and Table 5, respectively. They clearly indicate that $\|u - u_h\|_0 = \mathcal{O}(h^2)$, $\|\sigma - \sigma_h\|_{H(\operatorname{div})} = \mathcal{O}(h^2)$ for $k = 1$ and $\|u - u_h\|_0 = \mathcal{O}(h^4)$, $\|\sigma - \sigma_h\|_{H(\operatorname{div})} = \mathcal{O}(h^4)$ for $k = 3$, which agree with Theorem 3. In addition, we observe that convergence orders of the stress in L^2 -norm are also optimal.

In 3D case, the linear system of the Lagrange multiplier would be singular even on uniform grids. The singularity, however, does not affect the well-posedness of the original mixed system but only results in an SPSD system for the Lagrange multiplier, which can be solved efficiently by the Krylov solvers. More precisely, we use the conjugate gradient (CG) method with diagonal preconditioning to solve the SPSD system for the Lagrange multiplier and then compute the unique solution for the stress and the displacement element by element.

5.2 Iterative solver tests

In this subsection, we investigate the robustness of our iterative solvers with respect to both the mesh size h and Poisson's ratio $\tilde{\nu}$. In all the numerical experiments below, we

Table 6 Number of iterations of PCG: one-level multiplicative Schwarz preconditioner with subspaces supported on edges, elements, and vertex patches

Subdomains	$\tilde{\nu}$					
	0.49	0.499	0.4999	0.49999	0.499999	0.4999999
Edges	36	59	79	109	131	154
Elements	15	24	33	45	54	62
Vertex patches	10	12	13	13	14	14

choose the data such that the exact solution is given by (72). High-order discretization of $k = 2$ is applied on the uniform grids. The Lamé constants are set as $\tilde{\mu} = 1/2$ and

$$\tilde{\lambda} = \frac{\tilde{\nu}}{1 - 2\tilde{\nu}},$$

where $\tilde{\nu}$ represents the Poisson's ratio that goes to 0.5 when the material becomes increasingly incompressible.

We run the various preconditioning Conjugate Gradient (PCG) computations with zero initial guess and a stopping criterion whereby the relative residual is smaller than 10^{-6} . We verify the reasonableness of our choices for Schwarz smoother, intergrid transfer operator and coarse solvers in the following numerical experiments.

Example 3 (One-level Schwarz preconditioner) This example is to verify the $\tilde{\nu}$ -independent property of the Schwarz method on the fine grid. Clearly any local space defined on the vertex patch (edges that share the same vertex) belongs to one subspace defined in (41) at least. Hence, the corresponding Schwarz method would be uniform with respective to $\tilde{\nu}$. We also test the other two choices of the space decompositions with supported sets on edge patches and element patches, respectively.

Table 6 presents the number of iterations of PCG with symmetrized multiplicative Schwarz preconditioner for different decompositions. The mesh size is set as $h = 1/4$. Only the decomposition consisting of vertex patches provides a $\tilde{\nu}$ -independent method.

Example 4 (Two-level Schwarz preconditioners) We now validate the robustness of the two-level Schwarz preconditioner. We note that the \mathcal{P}_2 Lagrange finite element space W_H is used as coarse space due to its d.o.f. that preserve rigid-body motion as well as the moments on the edges, see Lemma 13. The fine grid $\mathcal{T}_h = \{K_h\}$ is refined uniformly from the coarse grid $\mathcal{T}_H = \{K_H\}$. Hence, the overlap is set as $\delta = h$ and the ratio $H/\delta = 2$. The intergrid transfer operator is defined as $I_H^h = Q_h \tilde{I}_H^h$ in (47).

Table 7 lists the number of iterations of PCG using the additive Schwarz preconditioner (43) and the corresponding symmetrized multiplicative Schwarz preconditioner. This result clearly shows the robustness of the Schwarz preconditioner in agreement with the Theorem 7.

Example 5 (Multilevel preconditioner) We test the scalability of a multilevel preconditioner. In this test, we use W_H (i.e., continuous space of piecewise $(\mathcal{P}_2)^2$) as the coarse space. The intergrid transfer operator and the overlapping subdomains and are

Table 7 Number of iterations of PCG: two-level additive Schwarz preconditioner (left) and symmetrized multiplicative Schwarz preconditioner (right)

$1/h$	\tilde{v}						
		0.49	0.499	0.4999	0.49999	0.499999	0.4999999
4	17, 3	18, 4	21, 4	23, 4	23, 4	23, 4	23, 4
8	17, 4	20, 4	25, 4	27, 5	28, 5	29, 5	29, 5
16	18, 4	20, 4	26, 5	28, 5	29, 5	29, 5	29, 5
32	18, 4	20, 4	25, 5	27, 5	28, 5	29, 5	29, 5

Table 8 Number of iterations of PCG, multilevel symmetrized multiplicative preconditioner

$1/h$	\tilde{v}						
		0.49	0.499	0.4999	0.49999	0.499999	0.4999999
4	4	5	5	5	5	5	5
8	4	6	7	7	7	7	7
16	5	6	7	7	7	7	7
32	5	6	7	7	7	7	7

the same as those of the second test. Instead of using an exact solver for A_H , we solve the coarse problem approximately using a W-2-2 cycle in [47]. Table 8 shows the uniform convergence of the multilevel symmetrized multiplicative preconditioner.

6 Concluding remarks

Motivated by the critical observation on the inter-element jump of the piecewise discontinuous symmetric-matrix-valued polynomials, we propose a family of hybridizable mixed finite elements for linear elasticity. These methods extend the works in [5, 11, 31, 35] by relaxing the continuity of the discrete stress on the grid vertices while preserving the symmetry and $H(\text{div})$ conformity in stress approximation. By hybridization, the solution cost for our discretization is dominated by the cost of solving the global system of the Lagrange multiplier. To develop robust solvers, we adopt the Schwarz method on the fine grid and the primal method as a coarse problem. The key to proving the uniform convergence of our iterative solvers is the construction of the interpolation operator I_h , which is stable with the approximation property (see Lemma 13). The new discretization, which preserves the physical structure of stress, along with the robust solver provides a new competitive approach for stress analysis in computational structure mechanics.

Acknowledgements The work of the first and third authors was supported in part by National Natural Science Foundation of China (NSFC) (Grant Nos. 91430215, 41390452) and by Beijing International Center for Mathematical Research of Peking University, China. The work of the second and third authors was supported in part by the DOE Grant DE-SC0009249 as part of the Collaboratory on Mathematics for Mesoscopic Modeling of Materials and by DOE Grant DE-SC0014400 and NSF Grant DMS-1522615.

Appendix A: Proof of Lemma 3 (construction of the bases of $\mathbb{R}(\mathcal{C})$ and $\mathbb{R}(\mathcal{C}^\perp)$)

Proof Denote the set of all $k+1$ degree Lagrange nodes in \mathcal{T}_h by $A_{h,k+1}$. For any $K \in \mathcal{T}_h$ and $a \in A_{h,k+1} \cap \bar{K}$, let φ_a^K be the Lagrange nodal basis in K , with zero extension in $\mathcal{T}_h \setminus K$. Further, for any $F \in \mathcal{F}_h^i$ and $a \in A_{h,k+1} \cap \bar{F}$, let ψ_a^F be the dual basis of the degree $k+1$ Lagrange basis such that

$$\langle \psi_{a'}^F, \varphi_a^K \rangle_F = \delta_{a,a'} \quad \text{and} \quad \psi_{a'}^F|_{\mathcal{F}_h \setminus F} = 0.$$

For any $a \in A_{h,k+1}$, define the local spaces

$$\begin{aligned} \Sigma_{h,k+1,a}^{-1} &:= \text{span}\{\varphi_a^K T_{ij} \mid 1 \leq i \leq j \leq n, \bar{K} \ni a\}, \\ M_{h,k+1,a} &:= \text{span}\{\psi_a^F e_i \mid 1 \leq i \leq n, F \in \mathcal{F}_h^i, \bar{F} \ni a\}, \end{aligned} \quad (73)$$

where $\{e_i \mid 1 \leq i \leq n\}$ is the basis of \mathbb{R}^n and $\{T_{ij} = \frac{1}{2}(e_i e_j^T + e_j e_i^T) \mid 1 \leq i \leq j \leq n\}$ is the basis of \mathbb{S} . Clearly,

$$\Sigma_{h,k+1}^{-1} = \bigoplus_{a \in A_{h,k+1}} \Sigma_{h,k+1,a}^{-1} \quad \text{and} \quad M_{h,k+1} = \bigoplus_{a \in A_{h,k+1}} M_{h,k+1,a}.$$

Moreover, if $a \neq a'$ and $\mu \in \mathcal{C}(\Sigma_{h,k+1,a}^{-1}) \cap \mathcal{C}(\Sigma_{h,k+1,a'}^{-1})$, then μ vanishes at all the Lagrange nodes on the faces. This implies that $\mu = 0$, namely

$$\mathcal{C}(\Sigma_{h,k+1,a}^{-1}) \cap \mathcal{C}(\Sigma_{h,k+1,a'}^{-1}) = \{0\} \quad \text{if } a \neq a'.$$

Hence, we have

$$\mathbb{R}(\mathcal{C}) = \mathcal{C}(\Sigma_{h,k+1}^{-1}) = \bigoplus_{a \in A_{h,k+1}} \mathcal{C}(\Sigma_{h,k+1,a}^{-1}). \quad (74)$$

Therefore, $\mathbb{R}(\mathcal{C})$ has local basis since $\mathcal{C}(\Sigma_{h,k+1,a}^{-1})$ is locally supported for any $a \in A_{h,k+1}$.

Next, we construct the local basis for $\mathbb{R}(\mathcal{C})^\perp$. Let

$$M_{h,k+1,a,\perp} := \left\{ \mu_a \in M_{h,k+1,a} \mid \langle \mu_a, [\tau_a] \rangle_{\mathcal{F}_h^i} = 0 \quad \forall \tau_a \in \Sigma_{h,k+1,a}^{-1} \right\}. \quad (75)$$

If $a \neq a'$, we further have

$$\langle \mu, \mathcal{C}\tau \rangle_{\mathcal{F}_h^i} = 0 \quad \forall \mu \in M_{h,k+1,a}, \tau \in \Sigma_{h,k+1,a'}^{-1}.$$

Hence, we have $M_{h,k+1,a,\perp} \subset \mathbb{R}(\mathcal{C})^\perp$ and

$$\mathbb{R}(\mathcal{C})^\perp = \bigoplus_{a \in A_{h,k}} M_{h,k+1,a,\perp}. \quad (76)$$

Therefore, the local basis $\{\psi_1, \psi_2, \dots, \psi_{N_2}\}$ of $R(\mathcal{C})^\perp$ comes from the union of the basis of $M_{h,k+1,a,\perp}$ for all $a \in A_{h,k}$. \square

In the proof of Lemma 3, we show the decomposition of $R(\mathcal{C})^\perp$ in (76) as the direct sum of $M_{h,k+1,a,\perp}$. Note that $M_{h,k+1,a,\perp}$ only involves the local basis associated with the Lagrange node a . Moreover, the dimension of $M_{h,k+1,a,\perp}$ only depends on the topology of the grid near the Lagrange node a , but does not depend on the degree of the polynomials k . Hence, we can use $M_{h,k+1,a,\perp}$ to characterize singular vertices for any spatial dimension:

Definition 1 The Lagrange node a is called *singular* if $M_{h,k+1,a,\perp}$ is a nontrivial set.

For 2D case, a direct calculation shows that $M_{h,k+1,a,\perp}$ is a nontrivial set if and only if the edges meeting at this vertex a fall on two straight lines. For 3D case, when a is a Lagrange node on the edge e , $M_{h,k+1,a,\perp}$ is a nontrivial set if and only if the faces meeting at this edge a fall on two planes. However, if a is a mesh vertex, it is difficult to describe the ordering of the element faces containing the vertex a . It is still an open problem to give a geometric description of the singular vertex in 3D case.

Appendix B: Proof of Lemma 6

Proof The basis of $M_{h,k+1,a,\perp}$ can be computed locally according to its definition (75). In particular, $M_{h,k+1,a,\perp}$ is nontrivial for the 2D case only if a is an interior singular vertex. Thus, if there is no interior singular vertex in T_h , then $R(\mathcal{C})^\perp = \{0\}$, or $M_{h,k+1} = R(\mathcal{C}) = \bigoplus_{a \in A_{h,k+1}} \mathcal{C}(\Sigma_{h,k+1,a}^{-1})$. Further, a direct calculation shows that

$$\mathcal{C}(\Sigma_{h,k+1,a}^{-1}) = \begin{cases} \text{span}\{\varphi_a^F e_i \mid 1 \leq i \leq 2, F \in \mathcal{F}_h^i, \bar{F} \ni a\} & a \in \bar{\mathcal{F}}_h^i, \\ \{0\} & a \notin \bar{\mathcal{F}}_h^i, \end{cases}$$

where φ_a^F denotes the Lagrange nodal basis on F . Therefore, we can choose a special basis of $R(\mathcal{C})$ as

$$M_{h,k+1} = \bigoplus_{a \in \bar{\mathcal{F}}_h^i \cap A_{h,k+1}} \text{span}\{\varphi_a^F e_i \mid 1 \leq i \leq 2, F \in \mathcal{F}_h^i, \bar{F} \ni a\}. \quad (77)$$

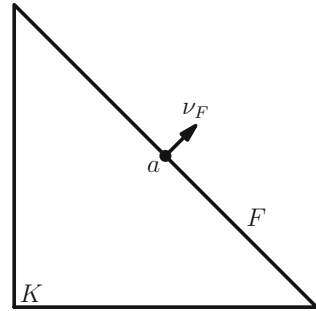
The mass matrix under the special basis (77) is the diagonal block matrix whose diagonal block entry is the local mass matrix under the Lagrange nodal basis on F . Hence, the mass matrix \mathbf{M} is well-conditioned because the local mass matrix is well conditioned for the Lagrange nodal basis, which gives rise to (36). This completes the proof. \square

Appendix C: Proof of Lemma 7

Proof In light of (74) in the proof of Lemma 6, there exists a Lagrange node $a \in A_{h,k+1}$ such that $\varphi_i \in \mathcal{C}(\Sigma_{h,k+1,a}^{-1})$. Further, we have

$$\varphi_i = \omega \varphi_a|_{\mathcal{F}_h},$$

Fig. 2 Internal Lagrange node on edge F



where φ_a is the Lagrange nodal basis function at the node a and $\omega \in L^2(\mathcal{F}; \mathbb{R}^2)$ is piecewise constant and $\text{supp}(\omega) \subset \{F \in \mathcal{F}_h^i \mid \bar{F} \ni a\}$. Next, we construct $\tau_i \in \Sigma_{h,k+1}^{-1}$ case by case according to the location of a . Clearly, if a is not located on the $\bar{\mathcal{F}}_h^i$, then $\mathcal{C}(\Sigma_{h,k+1,a}^{-1}) = \{0\}$. Hence, we only need to consider the following two cases: Internal Lagrange node on $F \in \mathcal{F}_h^i$, or vertex of \mathcal{T}_h . We first state a useful tool for the analysis: For any given vectors $v, w \in \mathbb{R}^2$, there exists $T \in \mathbb{S}$ such that

$$Tv = w \quad \text{and} \quad \|T\|_{l^2} \leq \sqrt{2} \frac{\|w\|_{l^2}}{\|v\|_{l^2}}. \quad (78)$$

A straightforward calculation shows that T in (78) can be chosen as

$$T = \frac{w_1}{\|v\|_{l^2}^2} \begin{pmatrix} v_1 & v_2 \\ v_2 & -v_1 \end{pmatrix} + \frac{w_2}{\|v\|_{l^2}^2} \begin{pmatrix} -v_2 & v_1 \\ v_1 & v_2 \end{pmatrix}.$$

Case 1: Internal Lagrange node of $F \in \mathcal{F}_h^i$. First, we select an element K such that $F \in \bar{K}$ (cf. Fig. 2). By virtue of (78), there exists $T \in \mathbb{S}$ such that

$$Tv_F = \omega|_F \quad \text{and} \quad \|T\|_{l^2} \lesssim \|\omega|_F\|_{l^2}.$$

From the definition of $\Sigma_{h,k+1,a}^{-1}$ in (73), let $\tau_i = \varphi_a^K T \in \Sigma_{h,k+1,a}^{-1}$. Then,

$$\begin{aligned} [\tau_i]_F &= \varphi_i|_F \quad \forall F \in \mathcal{F}_h \quad \text{and} \\ \|\tau_i\|_0^2 &= \|\varphi_a\|_{0,K}^2 \|T\|_{l^2}^2 \lesssim h \|\varphi_a\|_{0,F}^2 \|\omega|_F\|_{l^2}^2 = h \|\varphi_i\|_0^2. \end{aligned}$$

Case 2: Vertex of \mathcal{T}_h . Suppose that there are m (≥ 2) elements meeting at the vertex a . Since $\kappa \geq \kappa_0 > 0$, there exist two adjacent elements (without loss of generality, denoted by K_1 and K_2), such that the angles θ_1 and θ_2 satisfying $|\theta_1 + \theta_2 - \pi| \geq \kappa_0$, (cf. Fig. 3). The edges that contain a are denoted by F_j , $1 \leq j \leq m$ if a is an internal vertex, and $1 \leq j \leq m+1$ otherwise. If a is a boundary vertex, we further set $F_1, F_{m+1} \in \mathcal{F}_h^\partial$, which is feasible because $\kappa(a) \geq \kappa_0 > 0$.

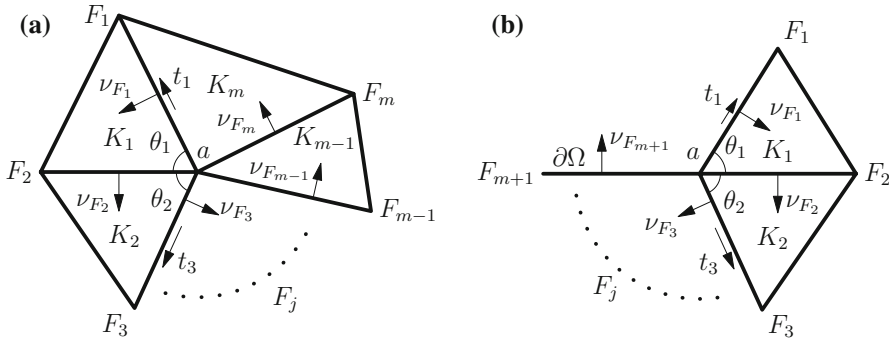


Fig. 3 Vertex of \mathcal{T}_h . **a** Internal vertex. **b** Boundary vertex

If a is an internal vertex, let $F_{m+1} = F_1$ and $\nu_{F_{m+1}} = \nu_{F_1}$. By virtue of (78), there exists $T_m \in \mathbb{S}$ such that

$$T_m \nu_{F_{m+1}} = \omega|_{F_{m+1}} \quad \text{and} \quad \|T_m\|_{l^2} \lesssim \|\omega|_{F_{m+1}}\|_{l^2}. \quad (79)$$

Note that $T_m = \mathbf{0} \in \mathbb{S}$ if a is a boundary vertex. Recursively for $j = m-1, m-2, \dots, 2$, there exist $T_j \in \mathbb{S}$ on K_j such that

$$\begin{aligned} T_j \nu_{F_{j+1}} &= \omega|_{F_{j+1}} + T_{j+1} \nu_{F_{j+1}} \quad \text{and} \\ \|T_j\|_{l^2} &\lesssim \|\omega|_{F_{j+1}}\|_{l^2} + \|T_{j+1}\|_{l^2} \lesssim \sum_{s=j}^{m+1} \|\omega|_{F_s}\|_{l^2}. \end{aligned} \quad (80)$$

Since $\omega|_{F_0} = 0$ if a is a boundary vertex, we simply set $T_1 = \mathbf{0} \in \mathbb{S}$.

Next, we find two symmetric matrices $\tilde{T}_1 = c_1 t_1 t_1^T$ and $\tilde{T}_2 = c_2 t_3 t_3^T$ on K_1 and K_2 , respectively. Here, t_1, t_3 are the unit tangential vectors of F_1 and F_3 , respectively (cf. Fig. 3). The coefficients c_1, c_2 are determined by

$$\tilde{T}_1 \nu_{F_2} - \tilde{T}_2 \nu_{F_2} = \omega|_{F_2} + T_2 \nu_{F_2}, \quad (81)$$

i.e.

$$-(t_1, t_3) \begin{pmatrix} c_1 \sin \theta_1 \\ c_2 \sin \theta_2 \end{pmatrix} = \omega|_{F_2} + T_2 \nu_{F_2}.$$

Since $|\theta_1 + \theta_2 - \pi| \geq \kappa_0$, we have $|\det(t_1, t_3)| = |t_1 \times t_3| = |\sin(\theta_1 + \theta_2)| \geq \sin(\kappa_0)$. Thus, the matrix (t_1, t_3) is invertible. Moreover, we have $|(t_1, t_3)^{-1}|_\infty \lesssim \sin^{-1}(\kappa_0)$ and, by the shape regularity of grids, $|\sin \theta_1|$ and $|\sin \theta_2|$ are bounded uniformly away from zero. Thus,

$$\|\tilde{T}_1\|_{l^2}^2 + \|\tilde{T}_2\|_{l^2}^2 \lesssim c_1^2 + c_2^2 \lesssim \sin^{-2}(\kappa_0) \|\omega|_{F_2} + T_2 \nu_{F_2}\|_{l^2}^2 \lesssim \sin^{-2}(\kappa_0) \sum_{j=1}^{m+1} \|\omega|_{F_j}\|_{l^2}^2.$$

In light of (79), (80), and (81), let

$$\boldsymbol{\tau}_i|_{K_j} = \begin{cases} \varphi_a^{K_j}(T_j + \tilde{T}_j) & j = 1, 2, \\ \varphi_a^{K_j} T_j & 3 \leq j \leq m. \end{cases} \quad (82)$$

Then, we have

$$[\boldsymbol{\tau}_i]|_F = \varphi_i|_F \quad \forall F \in \mathcal{F}_h, \quad \text{and} \quad \|\boldsymbol{\tau}_i\|_0^2 \lesssim h \sin^{-2}(\kappa_0) \|\varphi_i\|_0^2.$$

This completes the proof. \square

References

1. Adams, S., Cockburn, B.: A mixed finite element method for elasticity in three dimensions. *J. Sci. Comput.* **25**(3), 515–521 (2005)
2. Amara, M., Thomas, J.M.: Equilibrium finite elements for the linear elastic problem. *Numer. Math.* **33**(4), 367–383 (1979)
3. Antonietti, P.F., Verani, M., Zikatanov, L.: A two-level method for mimetic finite difference discretizations of elliptic problems. *Comput. Math. Appl.* **70**(11), 2674–2687 (2015)
4. Arnold, D.N., Awanou, G.: Rectangular mixed finite elements for elasticity. *Math. Models Methods Appl. Sci.* **15**(09), 1417–1429 (2005)
5. Arnold, D.N., Awanou, G., Winther, R.: Finite elements for symmetric tensors in three dimensions. *Math. Comput.* **77**(263), 1229–1251 (2008)
6. Arnold, D.N., Brezzi, F.: Mixed and nonconforming finite element methods: implementation, postprocessing and error estimates. *RAIRO-Modél. Math. et Anal. Numér.* **19**(1), 7–32 (1985)
7. Arnold, D.N., Douglas Jr., J., Gupta, C.P.: A family of higher order mixed finite element methods for plane elasticity. *Numer. Math.* **45**(1), 1–22 (1984)
8. Arnold, D.N., Falk, R., Winther, R.: Mixed finite element methods for linear elasticity with weakly imposed symmetry. *Math. Comput.* **76**(260), 1699–1723 (2007)
9. Arnold, D.N., Falk, R.S., Winther, R.: Finite element exterior calculus, homological techniques, and applications. *Acta Numer.* **15**(1), 1–155 (2006)
10. Arnold, D.N., Qin, J.: Quadratic velocity/linear pressure stokes elements. *Adv. Comput. Methods Partial Differ. Equ.* **7**, 28–34 (1992)
11. Arnold, D.N., Winther, R.: Mixed finite elements for elasticity. *Numer. Math.* **92**(3), 401–419 (2002)
12. Arnold, D.N., Winther, R.: Nonconforming mixed elements for elasticity. *Math. Models Methods Appl. Sci.* **13**(03), 295–307 (2003)
13. Awanou, G.: A rotated nonconforming rectangular mixed element for elasticity. *Calcolo* **46**(1), 49–60 (2009)
14. Boffi, D., Brezzi, F., Fortin, M.: Reduced symmetry elements in linear elasticity. *Commun. Pure Appl. Anal.* **8**(1), 95–121 (2009)
15. Brenner, S., Scott, R.: The Mathematical Theory of Finite Element Methods, vol. 15. Springer, London (2007)
16. Brenner, S.C.: Multigrid methods for parameter dependent problems. *RAIRO-Modél. Math. et Anal. Numér.* **30**(3), 265–297 (1996)
17. Brezzi, F., Douglas Jr., J., Marini, L.D.: Two families of mixed finite elements for second order elliptic problems. *Numer. Math.* **47**(2), 217–235 (1985)
18. Brezzi, F., Fortin, M.: Mixed and Hybrid Finite Element Methods, vol. 15. Springer, Berlin (2012)
19. Chen, L.: iFEM: An Innovative Finite Element Methods Package in MATLAB. University of Maryland, Preprint (2008)
20. Chen, L., Hu, J., Huang, X.: Fast Auxiliary Space Preconditioner for Linear Elasticity in Mixed Form. *Mathematics of Computation* (2017)
21. Cho, D., Xu, J., Zikatanov, L.: New estimates for the rate of convergence of the method of subspace corrections. *Numer. Math.: Theory Methods Appl.* **1**(1), 44–56 (2008)

22. Cockburn, B., Dubois, O., Gopalakrishnan, J., Tan, S.: Multigrid for an HDG method. *IMA J. Numer. Anal.* **34**(4), 1386–1425 (2014)
23. Cockburn, B., Gopalakrishnan, J., Guzmán, J.: A new elasticity element made for enforcing weak stress symmetry. *Math. Comput.* **79**(271), 1331–1349 (2010)
24. Cockburn, B., Gopalakrishnan, J., Lazarov, R.: Unified hybridization of discontinuous Galerkin, mixed, and continuous Galerkin methods for second order elliptic problems. *SIAM J. Numer. Anal.* **47**(2), 1319–1365 (2009)
25. de Dios, B.A., Georgiev, I., Kraus, J., Zikatanov, L.: A subspace correction method for discontinuous galerkin discretizations of linear elasticity equations. *ESAIM: Math. Model. Numer. Anal.* **47**(5), 1315–1333 (2013)
26. Gopalakrishnan, J.: A Schwarz preconditioner for a hybridized mixed method. *Comput. Methods Appl. Math. Comput. Methods Appl. Math.* **3**(1), 116–134 (2003)
27. Gopalakrishnan, J., Guzmán, J.: Symmetric nonconforming mixed finite elements for linear elasticity. *SIAM J. Numer. Anal.* **49**(4), 1504–1520 (2011)
28. Gopalakrishnan, J., Tan, S.: A convergent multigrid cycle for the hybridized mixed method. *Numer. Linear Algebra Appl.* **16**(9), 689–714 (2009)
29. Guzmán, J.: A unified analysis of several mixed methods for elasticity with weak stress symmetry. *J. Sci. Comput.* **44**(2), 156–169 (2010)
30. Hong, Q., Kraus, J., Xu, J., Zikatanov, L.: A robust multigrid method for discontinuous Galerkin discretizations of stokes and linear elasticity equations. *Numer. Math.* **132**(1), 23–49 (2016)
31. Hu, J.: Finite element approximations of symmetric tensors on simplicial grids in \mathbb{R}^n : the higher order case. *J. Comput. Math.* **33**(3), 283–296 (2015)
32. Hu, J.: A new family of efficient conforming mixed finite elements on both rectangular and cuboid meshes for linear elasticity in the symmetric formulation. *SIAM J. Numer. Anal.* **53**(3), 1438–1463 (2015)
33. Hu, J., Shi, Z.C.: Lower order rectangular nonconforming mixed finite elements for plane elasticity. *SIAM J. Numer. Anal.* **46**(1), 88–102 (2007)
34. Hu, J., Zhang, S.: A family of conforming mixed finite elements for linear elasticity on triangular grids. arXiv preprint [arXiv:1406.7457](https://arxiv.org/abs/1406.7457) (2014)
35. Hu, J., Zhang, S.: A family of symmetric mixed finite elements for linear elasticity on tetrahedral grids. *Sci. China Math.* **58**(2), 297–307 (2015)
36. Hu, J., Zhang, S.: Finite element approximations of symmetric tensors on simplicial grids in \mathbb{R}^n : the lower order case. *Math. Models Methods Appl. Sci.* **26**(09), 1649–1669 (2016)
37. Hu, X., Wu, S., Wu, X.H., Xu, J., Zhang, C.S., Zhang, S., Zikatanov, L.: Combined preconditioning with applications in reservoir simulation. *Multiscale Model. Simul.* **11**(2), 507–521 (2013)
38. Johnson, C., Mercier, B.: Some equilibrium finite element methods for two-dimensional elasticity problems. *Numer. Math.* **30**(1), 103–116 (1978)
39. Lee, Y.J., Wu, J., Chen, J.: Robust multigrid method for the planar linear elasticity problems. *Numer. Math.* **113**(3), 473–496 (2009)
40. Li, B., Xie, X.: Analysis of a family of HDG methods for second order elliptic problems. *J. Comput. Appl. Math.* **307**, 37–51 (2016)
41. Li, B., Xie, X.: BPX preconditioner for nonstandard finite element methods for diffusion problems. *SIAM J. Numer. Anal.* **54**(2), 1147–1168 (2016)
42. Man, H.Y., Hu, J., Shi, Z.C.: Lower order rectangular nonconforming mixed finite element for the three-dimensional elasticity problem. *Math. Models Methods Appl. Sci.* **19**(01), 51–65 (2009)
43. Morgan, J., Scott, R.: A nodal basis for C^1 piecewise polynomials of degree $n \geq 5$. *Math. Comput.* **29**(131), 736–740 (1975)
44. Morley, M.E.: A family of mixed finite elements for linear elasticity. *Numer. Math.* **55**(6), 633–666 (1989)
45. Qiu, W., Demkowicz, L.: Mixed hp-finite element method for linear elasticity with weakly imposed symmetry. *Comput. Methods Appl. Mech. Eng.* **198**(47), 3682–3701 (2009)
46. Qiu, W., Shen, J., Shi, K.: An HDG method for linear elasticity with strong symmetric stresses. *Math. Comput.* **87**(309), 69–93 (2018)
47. Schöberl, J.: Multigrid methods for a parameter dependent problem in primal variables. *Numer. Math.* **84**(1), 97–119 (1999)
48. Schöberl, J.: Robust multigrid methods for parameter dependent problems. Ph.D dissertation, Johannes Kepler Universität Linz (1999)

49. Scott, L.R., Vogelius, M.: Norm estimates for a maximal right inverse of the divergence operator in spaces of piecewise polynomials. *RAIRO-Modél. Math. et Anal. Numér.* **19**(1), 111–143 (1985)
50. Scott, L.R., Zhang, S.: Finite element interpolation of nonsmooth functions satisfying boundary conditions. *Math. Comput.* **54**(190), 483–493 (1990)
51. Soon, S.C., Cockburn, B., Stolarski, H.K.: A hybridizable discontinuous Galerkin method for linear elasticity. *Int. J. Numer. Methods Eng.* **80**(8), 1058–1092 (2009)
52. Toselli, A., Widlund, O.: Domain Decomposition Methods: Algorithms and Theory, vol. 34. Springer, London (2005)
53. Wu, S., Gong, S., Xu, J.: Interior penalty mixed finite element methods of any order in any dimension for linear elasticity with strongly symmetric stress tensor. *Math. Models Methods Appl. Sci.* **27**(14), 2711–2743 (2017)
54. Xu, J.: Iterative methods by space decomposition and subspace correction. *SIAM Rev.* **34**(4), 581–613 (1992)
55. Yi, S.Y.: Nonconforming mixed finite element methods for linear elasticity using rectangular elements in two and three dimensions. *Calcolo* **42**(2), 115–133 (2005)
56. Yi, S.Y.: A new nonconforming mixed finite element method for linear elasticity. *Math. Models Methods Appl. Sci.* **16**(07), 979–999 (2006)
57. Zhang, S.: A new family of stable mixed finite elements for the 3D Stokes equations. *Math. Comput.* **74**(250), 543–554 (2005)